Flood Hazard and Risk Mapping Using Multicriteria Evaluation and Geospatial Technology:

A Case of Jimma town Oromia Region, Ethiopia

By

Abraham Taye Lema

A Thesis Submitted to

Department of Geomatics Engineering

School of Civil and Architecture Engineering

Presented in Partial Fulfillment of the requirements for the award of the degree of Masters of Science in Geoinformatics Engineering, Specialization in Geoinformatics.

Office of Graduate Studies

Adama Science and Technology University

June 2021

Adama, Ethiopia

Flood Hazard and Risk Mapping Using Multicriteria Evaluation and Geospatial Technology:

A Case of Jimma town Oromia Region, Ethiopia

By

Abraham Taye Lemma

Advisor: Tilahun Erduno (Ph.D.)

Co-Advisor: Dereje Birhanu (Ph.D.)

A Thesis Submitted to

The Department of Geomatics Engineering

School of Civil and Architecture Engineering

Presented in Partial Fulfillment of the requirements for the award of the degree of Masters of Science in Geoinformatics Engineering Specialization in Geoinformatics.

Office of Graduate Studies

Adama Science and Technology University

June 2021

Adama, Ethiopia

APPROVAL SHEET

We, the advisors of the thesis entitled, “Flood Hazard and Risk Mapping Using Multicriteria Evaluation and Geospatial Technology” and developed by Abraham Taye, hereby certify that the recommendation and suggestions made by the board of examiners are appropriately incorporated into the final version of the thesis.

Tilahun Erduno (Ph.D.)	______________	____________
Advisor	Signature	Date
Dereje Birhanu (Ph.D.)	______________	____________
Co-Advisor	Signature	Date

We, the undersigned, members of the Board of Examiners of the thesis by Abraham Taye have read and evaluated the thesis entitled, “Flood Hazard and Risk Mapping Using Multicriteria Evaluation and Geospatial Technology” and examined the candidate during the open defense. This is, therefore, to certify that the thesis is accepted for partial fulfillment of the requirement of the degree of Master of Science in Geoinformatics Engineering.

Chairman, Department Graduate Committee	Signature	Date
Internal Examiner	Signature	Date
External Examiner	Signature	Date

Finally, approval and acceptance of the thesis is contingent upon submission of its final copy to the Office of Postgraduate Studies (OPGS) through the Department Graduate Council (DGC) and School Graduate Committee (SGC).

Department Head	Signature	Date
School Dean	Signature	Date
Office of Postgraduate Studies, Dean	Signature	Date

DECLARATION

I the undersigned, declare that the thesis entitled "Flood Hazard and Risk Mapping Using Multicriteria Evaluation and Geospatial Technology: A Case of Jimma town Oromia Region, Ethiopia" has been carried out by me under the supervision of Dr. Tilahun Erduno and Dr. Dereje Birhanu, Department of Geomatics Engineering, Adama Science and Technology University, during the year 2020-2021 as a part of Master of Science program in Geoinformatics Engineering.

Abraham Taye	____________________	_________________
Candidate	Signature	Date

RECOMMENDATION

We, the advisors of this thesis, hereby certify that we have read the revised version of the thesis entitled "Flood Hazard and Risk Mapping Using Multicriteria Evaluation and Geospatial Technology: A Case of Jimma town Oromia Region, Ethiopia" prepared under our guidance by Abraham Taye for the partial fulfillment of the award of the Degree of Master of Science in Geoinformatics Engineering, Adama Science and Technology University, Adama, Ethiopia. Therefore, we recommend the submission of the revised version of the thesis to the department following the applicable procedures.

Dr. Tilahun Erduno	_________________	___________-____
Advisor	Signature	Date
Dr. Dereje Birhanu	___________________	________________
Co-Advisor	Signature	Date

ACKNOWLEDGMENTS

First of all, I would like to thank the 'Almighty God' who made it possible, to begin and finish this work successfully. I do not have adequate words to express my feeling to my advisor Dr. Tilahun Erduno and Dr. Dereje Birhanu whose benevolent guidance and constant encouragement helped me to complete the present thesis work successfully. I am grateful to Mr. Gemachu, Head of the Geomatics Engineering Department, Adama Science and Technology University and other members of the department for their help, encouragement and cooperation which gave me enough strength to carry out the present research study. I am also thankful to the Ministry of Agriculture, National Metrological Agency and Central Statistical Agency for their support, Jimma town municipality, and other communities in Jimma town and provision of necessary data and information related to the thesis until the completion of my work. Finally, I would also like to express my gratitude to my friends, relatives who directly and indirectly made it possible for me to complete this thesis in financially and by any means of support.

TABLE OF CONTENTS

LIST OF TABLES

LIST OF FIGURES

Figure Figure title Page

ACRONOYM

AHP	Analytical Hierarchy Process
ALOS	Advanced Land Observational Satellite
CSA	Central Statistics Agency
DEM	Digital Elevation Model
DPPA	Disaster Preparedness and Prevention Agency
ETM	Enhanced Thematic Mapper
EMA	Ethiopian Mapping Agency
ERDAS	Earth Resources Data Analysis System
ESA	European space Agency
ESRI	Environmental System Research Institute
GPS	Global Positioning System
JAXA	Japan Aerospace Exploration Agency
LULC	Land Use / Land Cover
MCE	Multi Criteria Evaluation
NGO	Non-Governmental Organization
NMA	National Meteorological Agency
RMSE	Root mean Square Error
UNOCHA	United Nation Office for the Coordination of Humanitarian Affairs
UTM	Universal Transverse Mercator
WLC	Weighted Linear Combination

Abstract

Floods are one of the world's most common and devastating natural disasters, claiming lives and causing severe economic damage throughout the world. The flooding behavior has been changed due to how humans are using the existing land. Inadequate drainage systems and different activities including deforestation are increasing the magnitude of the flood. Jimma town is one of the floods affected areas in the Oromia region, especially areas around the river. Locally, Jimma city is drained by two perennial rivers, namely Awetu and Kito, which will be combined near Dedo bridge located towards the southwest tip of the city and pass through Boye Swamp before they join the Gilgel Gibe River. Awitu River is one of the main causes of the previous flood hazard in the study area. Due to the quick increment of the population, individuals are misusing the normal vegetation for different purposes, which has lead to deforestation and vulnerability to different natural hazards including floods. Thus, to manage such a problem, a detailed understanding of hazard identification or hazard-prone area delineation is very crucial. Therefore, this study was carried out to prepare the flood hazard and flood risk mapping in Jimma town using the Multi-Criteria Evaluation technique and Geospatial technologies. Eight flood causative factors including rainfall, drainage density, slope, elevation, soil type, topographic wetness index, distance from the river were developed in the GIS environment and land use land cover in Remote Sensing environment using ERDAS Imagine software. Then, the weighted overlay MCE technique was used to produce a flood hazard map depending on the Analytical hierarchy process (AHP) pairwise comparison of eigenvector value. IDRIS software was used to compute the eigenvector to derive the weight of each factor. To prepare a flood risk map of the study area, flood hazard map, population density, and land use land cover layer were overlaid. The findings of the study revealed that 6.81% and 28.11% of the town is under respectively very high to high flood hazard zone. Therefore, the study will help the concerned authorities to formulate their development strategies according to the available flood hazard in the area.

Keywords: *GIS, Remote Sensing, Jimma town, MCE, Flood Hazard,*

CHAPTER ONE; INTRODUCTION

1.1 Background to the Study

A flood occurs when water overflows and submerges normally dry land. Floods are one of the world's most common and devastating natural disasters, claiming lives and wreaking havoc on economies around the globe (Kumar & Sonam, 2020). Flood risks are expected to persist in the future, and with the onset of climate change, flood intensity and frequency will pose a threat to many parts of the globe (Jonkman & Dawson, 2012). According to Brunner (2018), extreme climate change has a significant impact on the frequency of floods, as well as their dynamics, rapidness, and destructiveness around the world. Climate change has an impact on the amount of water that falls into the wadi system and, as a result, the amount of runoff. Other geographical factors, such as topography, geomorphology, and morphometry, have an impact on the severity of the floods.

Flood casualties and damage are also on the rise in many areas as a result of social and economic development, which puts pressure on land use, such as through urbanization. Flooding is expected to become more common and severe as a result of climate change, severe weather in the form of heavy rains, and river discharge conditions (Dinh et al., 2012). As a result of the current trend and future flood risk scenarios, accurate spatial and temporal information on flood hazards and risks is required. As reported by Rahmati (2016), heavy convective rainfall often results in flooding in urban areas. Conversion of agricultural land, natural vegetation, and wetlands to built-up environments, as well as construction on natural drainages and an increase in the population of those living in flood-prone areas like flood plains and river beds, are all consequences of urbanization. Aside from population growth and the accumulation of valuable assets, climate change has increased the frequency and magnitude of floods (Ouma & Tateishi, 2014). In addition to population growth and the continued accumulation of valuable assets, climate change is expected to increase the frequency and magnitude of floods in the future, thereby exacerbating the existing flood risk in urban areas (Ouma & Tateishi, 2014).

According to this scenario, urban areas, in particular, face a disproportionately high flood risk due to their high population density, multiple economic activities, and numerous infrastructure and property values, all of which obstruct natural infiltration processes. Flood is causing many damages in Ethiopia due to different reasons such as lack of appropriate drainage system, river outflow, and heavy rainfall in the rainiest months between June and September. According to the National Meteorology Agency's weather forecast for September 2020, in most parts of the country, including Tigray, Benishangul Gumuz, Gambella, Jimma, East and West Gojjam, and North Shewa, the kiremt (summer) rain is expected to continue. According to the latest National Disaster Risk Management Commission (NDRMC) reports, floods have affected nearly 1,017,854 people and displaced 292,863 people across the country. Flood in afar especially affected most of the agricultural and farmlands and caused unexpected losses of human life and economic crisis (UNOCHA 2020).

Land inundation from heavy rainfall, river outflow, climate change, blockage of drainages with refuse, construction of buildings across drainages, inadequate drainage networks, and population growth in urban areas are all factors that contribute to flood disasters in Ethiopia. These factors do not act in isolation, and flood disasters are usually the result of a combination of them. Furthermore, urbanization leads to the conversion of agricultural land, natural vegetation, and wetlands to built-up environments, as well as construction on natural drainage systems and an increase in the population of people living in flood-prone areas like flood plains and river beds. (Akintoye et al., 2016).

In Jimma town, there is the exploitation of natural vegetation and expansion of cultivation as a result of the rapid growth of the population, resulting in land degradation and ecosystem deterioration. Locally, Jimma town is drained by two perennial rivers, Awetu and Kito, which unite near Dedo bridge on the town's southwest tip and flow through Boye Swamp before joining the Gilgel Gibe River. Awitu River flows down from the higher mountainous watershed, bisecting Jimma town in two, and Kito River flows along the city's western edge. Awitu River was one of the main reasons for flood hazard occurred in a previous flood event in Jimma town.

The town has diverse topography ranging from very flat to mountainous. The city's northern section is built on a series of hills or escarpments, with an undulating topography that gradually increases in slope to the north, eventually forming highlands that begin to decline further north in the hinterland districts. The core areas of the city's southern part, on the other hand, are mostly located on a low-elevation alluvial plain, with a slope that continues to decrease to the south and southeast. The town's topography, as well as the presence of rivers, are expected to contribute to the town's flood risk. To be able to prepare for disasters, adequate geographic information on hazards and vulnerable areas is required. Hazard risk vulnerability mapping is one of the most crucial steps in disaster risk reduction because it identifies disaster-prone areas so that disaster risk management can be planned (Tegegne et al., 2018). Remote sensing imagery and geographic information systems (GIS) can be very useful in identifying the spatial component of floods for management. Remote sensing provides a comprehensive picture of the spatial distribution and dynamics of hydrological events like flooding and erosion. They are used to quantify the land area and infrastructure affected by flooding and erosion, as well as to measure and monitor the extent of flooded areas (Ehiorobo & Izinyon, 2011).

Flood disaster mitigation can only be successful if detailed information about the spatial distribution, expected frequency, character, and magnitude of hazardous events in a given area, as well as the vulnerabilities of people, buildings, infrastructure, and economic activities in a potentially hazardous area, is obtained. Currently, spatial techniques, which are only available in GIS platforms, are gaining popularity among hazard mapping professionals (Hadipour et al., 2020). In terms of magnitude, frequency, and extent of floods at the basin scale, hydrological and hydrodynamic models are widely used (Kuldeep et al., 2016). Nonetheless, applying hydrodynamic models in limited-data situations and at the administrative level is a challenging task. As a result, assessing the magnitude of hazard using an index-based approach that combines critical parameters is a viable option. Quantitative approaches, such as the idea of ranking and weighting methods, are frequently used in a GIS environment. MCE – the goal of the decision-making tool is to compare and rank alternatives and assess their consequences based on a set of criteria. GIS-based Multi-criteria evaluation methods have been used by many researchers for flood hazard and risk mapping for a batter flood hazard management. Bulti (2017) assessed flood risk in Adama city using GIS-based multi-criteria evaluation methods. the research assessed all three dimensions of flood risk level in Adama City using a multi-criteria approach.

Nigusse (2019) utilized GIS and Remote Sensing technologies and MCDA for Flood Hazard and Flood Risk Vulnerability Mapping around Adigrat, Tigray Region, Northern Ethiopia. Ogato (2020) used (GIS)-Based multicriteria analysis method to analyze flooding hazards and risk in Ambo Town and its watershed. The purpose of their study was to analyze flooding hazard and risk from Geographic Information Systems (GIS)-based multicriteria perspective in Ambo town and its watershed and propose strategic measures for sustainable flooding disaster risk management in an urban watershed. Rimba (2017) used the GIS-Based Analytical Hierarchy Process for physical flood vulnerability mapping. Their Research involved the integration of Remote sensing data, the Geographic Information System method, and Analytical Hierarchy Process calculation to determine the physical flood-vulnerable area in Okazaki City.

Flood hazards cannot be eliminated, but they can be reduced in terms of risk and damage. The amount of flood information available and knowledge of the areas that are likely to be affected during a flood event will both play a role in reducing the risk of flooding (Mohamed & El-Raey, 2020). As a result, it is critical to employ modern technology in developing measures that will assist relevant authorities and relief agencies in identifying flood-prone areas and planning for future flooding events.

Determining the flood-prone area is important for effective flood mitigations. This study was conducted to prepare the flood hazard and risk map of Jimma town by using a multi-criteria evaluation method and GIS weighted overlay analysis by integrating Remote sensing images such as, ALOS PALSAR DEM and ESAs sentinel 2 images that are used for flood causative factor development. The accuracy of spatial analysis in a GIS environment is hardly affected by the accuracy and reliability of the input data. Thus, for this study, to improve the accuracy of the spatial dataset, these two (ALOS PALSAR DEM and ESAs sentinel 2 images) relatively high-resolution satellite images were used to derive flood causative factors.

1.2 Statement of the problem

Jimma town especially areas within the river basins are faced with flooding to the extent that damages are caused to human lives and other properties, whenever it rained heavily. Due to the topography of the town, rivers and some blocked drainage systems overflow their banks within the town causing devastating floods which result in the destruction of properties, lives, and other facilities which include damaging business shops and other houses of the residents within. the town. Due to the quick increment of the population, individuals are misusing the normal vegetation for different purposes, which has lead to deforestation and vulnerability to different natural hazards including floods. In 2006, about 150 households were displaced and suffered by floods frequently occurring throughout the year (UNOCHA, 2006). Some portions of the town's settlements and other landed properties were flooded after torrential rains (or intense rainfall) causing a runoff outflow of the Awitu river. The spatial distribution of the flood in the study area is rarely identified. The city's administrations and natural hazard management teams consider the flood plain areas are only those areas near to the river. No research was done to identify the flood-prone areas except the research that has been done by (Abdissa & Gudu, 2019) to model the Awitu river sub-basin. The research was focus only on modeling the Awitu river by using HEC RAS hydraulic modeling and DEM. It does not identify other parts of the study area which may be vulnerable to the flood. Hence to effectively handle the dynamics of flood disasters and to identify the flood-prone areas in the town, there is the need to find a geospatial method of identifying and mapping potential flood risk zones. Thus, the use of multi-criteria decision analysis with high resolution ALOS PALSAR DEM and GIS for spatial analyses and identifying flood-prone zones within the study area will serve as a valuable tool in the proper management of this devastating environmental hazard which affects most urban areas.

1.3 Objectives

The general objective of this research is to carry out a flood hazard and risk mapping for Jimma town using Geographic information system-based multi-criteria decision analysis. The following specific objectives are linked to the above-mentioned General objective::

- ✓ To identify the physical factors that contribute to a flood disaster.
- ✓ To produce a flood hazard map of the study area.
- ✓ To prepare a flood risk map and analyze the risk of a flood in the study area.

1.4 Research Question

The study is aimed to answer the following leading questions

- What are the main flood causative factors in the study area?
- How flood vulnerable area mapping is conducted.
- What are the levels of flood hazard, and risk in the study area?

1.5 Significance of the study

Before this study there was no detailed investigation had been conducted for this study area, the output or findings can serve as a basis to give more detailed information about the flood vulnerable areas, the clue for further investigation in preparation of planning, and flood hazard-prone area delineation. Jimma town municipality will use the outcome of this research for land use planning, environmental planning, land management, strategic urban expansion, construction of public service including hospitals, sports field, school, road and recommend policymakers and concerning government agents. The regional Disaster Risk Management task force also be benefited from this study for future Hazard preparedness. Environmental and educational planners, as well as environmental resource protection organizations, can benefit from this study. It also helps to have a better understanding of related training required for farmers in the area. Again, nongovernmental organizations (NGOs) and insurance companies will use the findings of this study to assist people living in flood-prone areas.

1.6 Scope of the study

The scope of the study was limited to Jimma town. The study was focused on flood vulnerability mapping of Jimma town using a multi-criteria evaluation method and GIS overlay analysis. The study comprises organizing the essential materials and procedures for conducting the study, identifying factors, mapping, a flood risk map for Jimma town using the MCE technique in a GIS setting. The Jimma town flood hazard and risk mapping in this study used the land use/land cover classes, topographic wetness index, drainage network, elevation, slope, rainfall, soil type, proximity to the river, and population statistics as input parameters (factors).

1.7 Organization of the thesis

The first chapter covers the thesis's introductory material, such as the problem statement, study objectives, research questions, significance, and scope of the study. The second chapter includes a review of related literature which are relevant to the research topic such as, publications, research, booklets and flood risk mapping related notes which are relevant to the thesis. Whereas, the third chapter provides materials and methods, details about the background of the study area such as physical settings including location, topography, soil types, climate and population. In addition, the materials describe detail about the data and software required for this study. In addition, the research methodology and procedures used to collect data are described in detail. The fourth chapter discusses data collection and analysis, as well as factors to be developed for flood hazard and risk mapping. Chapter 5 examines the outcome and discussion, which includes all of the output discussions of flood hazard, risk. Finally, Chapter six gives a conclusion and possible recommendation on the results of the study.

CHAPTER TWO; LITERATURE REVIEW

This chapter explores both theoretical and empirical frameworks. A Comprehensive Review of flood vulnerability mapping using geographic information system based multi-criteria evaluation method.

2.1 Theoretical Framework

A flood is an overflowing or irruption of a great body of water over land in a built-up area not usually submerged (Jonkman & Dawson, 2012). Floods are natural occurrences, but they become a source of concern when they exceed the coping capacities of affected communities, causing death and property damage. Globally floods are the most frequently occurring destructive natural event affecting both rural and urban settlements, (Kumar & Sonam, 2020)

The term "flood damage" encompasses all types of damage caused by flooding. It encompasses a wide range of negative effects on humans, their health, and their belonging on public infrastructure, cultural heritage, the ecological system, industrial production, and the economy's competitiveness (Singh et al., 2021). Flood damage is sometimes different, but it is usually divided into two categories: direct and indirect damages, and tangible and intangible damages. The research work of (Meyer & Messner, 2005) explains that direct flood damages cover all varieties of harms that relate to the immediate physical contact of food water to human property, and the environment. Damage to buildings, economic assets, loss of standing crops and cattle in agriculture, loss of human life, immediate health consequences, and loss of ecological goods are all examples of this.

Indirect flood damages are those incurred as a result of the economy's physical and economic linkages being disrupted, as well as the additional costs of emergency and other actions taken to avoid flood damage and other losses. However, tangible damages are those that can be quantified in monetary terms, such as lost production, whereas intangible damages, such as casualties, health effects, and damages to ecological goods that are not traded on the market, are more difficult to quantify in monetary terms (Meyer & Messner, 2005).

2.2 Flood in Global perspective

According to Danumah (2016) flood occurs when the flow of a stream becomes so great that it exceeds the capacity of its channels and overflows its banks. They also mentioned the situation in June 2008, when torrential rains across the American Midwest caused massive flooding, with many cities in Lowa, Wisconsin, Illinois, and Indiana experiencing their highest water level rise in over a century. The overflowing Cedar River, for example, flooded almost the entire downtown of Cedar Rapids, Lowa. (Jiang et al., 2018) also identified a major flood disaster in China, which impacted the urban population of Dongguan City, which is located in rapidly urbanizing southern China. In addition, the Pearl River Delta Area cities were flooded, resulting in serious casualties and property losses(Fernandez et al., 2016).

2.3 Flooding in Ethiopia

Floods are a type of extreme natural weather event that occurs when a large amount of surface water overflows onto land that is not always flooded (Akintoye et al., 2016). It is regarded as one of the worst natural disasters, causing half of the global damage to infrastructure. Floods have cost societies more than $250 billion in damages, and flood intensity and frequency are increasing around the world.

In Somalia, Oromia, Afar, SNNP, and Dire Dawa, strong and sustained rains caused flooding and landslides in April and May 2020. Floods have harmed almost 470,163 individuals and displaced 301,284 people across the country, according to the latest National Disaster Risk Management Commission (NDRMC) estimates. On 24 April, flash floods in Dire Dawa killed four people and damaged 53 houses (completely) and 212 houses (partially); on 25 April, river overflow damaged social infrastructure and affected livestock in Jinka town, SNNP; and on 25/26 April, flash floods in Erer, Sitti, Nogob, and Korahe zones, Somali region, affected 34,507 households and displaced 15,195 households. The flood on May 4 resulted in the total collapse of the main bridges connecting Hudet and Negalle, as well as Mubarak and Filtu. In addition, the rains made it difficult to travel to rural areas within the Dawa zone. (UNOCHA2020).

In total, 151,828 people have been displaced by recent floods (July and August 2020), with 100,176 individuals displaced as of mid-August, including 40,731 people impacted in Afar, 20,868 people displaced in Somalia, and 40,731 people displaced in Ethiopia, 1,125 people displaced in Oromia (excluding the 141 people displaced by a landslide in East Wollega zone), 25,703 people displaced in SNNP, and 11,749 people displaced in Gambella (UNOCHA 2020).

2.3.1 Factors of flooding in Ethiopia

The flood can occur due to natural phenomena and human activities. Streamflow, and thus the risk of flooding, is influenced by a variety of factors. The amount and type of precipitation, the nature and condition of the drainage basin, and the climate are the most important factors. Severe thunderstorms, tornadoes, tropical and extratropical cyclones (many of which can be exacerbated by the El-Nino phenomenon), monsoons, ice jams, and reservoir structural failure are all examples of climatic conditions (Singh et al., 2021). According to (Paquette & Lowry, 2012) flooding is most commonly caused by heavy rainfall when natural watercourses are unable to transport the excess water; however, floods are not always caused by heavy rainfall. Even in dry weather, a dam failure can cause flooding in a downstream area.

Floods can also occur as a result of the backflow of water from a flooding river without any rains falling, which was the case in Namibia in the Caprivi region in 2004 (Sanyal & Lu, 2005). Factors that influence whether a flood will occur, include volume, spatial distribution, intensity and duration of rainfall over a Catchment, the capacity of the watercourse or stream network to convey runoff; Catchment and weather conditions before a rainfall event; ground cover; topography and tidal influences (Gashaw & Legesse, 2011). Streamflow at any given point in a channel depends on the interaction of some factors, the most important of which are: distribution, intensity and duration of precipitation, vegetative cover, soil type, and geology of an area and topography; which includes elevation, slope, and channel characteristics (Dinh et al., 2012).

Poor land use can impact water resources by altering the hydrology (runoff, infiltration, and recharge rates) and increase soil erosion leading to increased sediment transport and deposition (Tapia-Silva et al., 2011). Because soils are formed by the rock types found in a given area, geology has a direct impact on the rate of water infiltration (deep percolation). The capacity of soil infiltration is influenced by land cover. Runoff is typically low in areas with a high percentage of vegetation cover because vegetated areas allow high infiltration until the earth is saturated because runoff is spread over a long period, whereas bare ground is expected to have increased overland runoff (Tapia-Silva et al., 2011).

There is evidence that land-use changes influence the hydrological regime of various river basins (Kumar & Sonam, 2020) which triggers the risk of flooding as a result of increased runoff and subsequent flood levels especially where vegetation is removed to make room for settlement or agriculture. All of the above factors are the main causes of the flood in different parts of the world including Ethiopia.

2.3.2 *Types of floods in Ethiopia*

The most common types of floods in Ethiopia are riverine, rain-induced flash floods, and floods that occur as a result of dam failure (Dereje 2017). Riverine flooding is a type of flooding that happens in low-lying areas near streams and rivers. A flash flood is a localized flood with a relatively high peak discharge that lasts for a short period of time (typically less than six hours) and is usually triggered by heavy rainfall in the immediate area with little or no advance warning (Miller, 1997). Flash floods can occur during a large storm, during a drought, or when heavy rains fall on very dry, hard ground that the water cannot penetrate, and they can occur practically everywhere. Despite their confined nature, flash floods pose a high risk of human death and property damage due to their unpredictability and short duration (Miller, 1997). The drainage system's capacity is insufficient to deal with the downpour in time during flash floods. Even if a region has never been flooded before, it is susceptible to future flooding. During flash floods, the drainage system's capacity is insufficient to deal with the downpour in time. Even if an area has never been flooded before, it is not immune to flooding in the future.

2.3.3 *Flooding in Jimma town*

The Awitu river has historical events of flooding in Jimma town. The flood in 2006 was mainly caused due to the high rainfall intensity and the lack of embankments along the Awitu River. On August 7, 2006, the Awitu River overflowed and flooded parts of town. Many low-elevation areas of the town were flooded, in addition to areas affected by a flood from the Awitu river. According to the United Nations Office for the Coordination of Humanitarian Affairs, about 150 households have been displaced as a result of floods that occur throughout the year UNOCHA (2006). Poor people living in a nearby stretch of the floodplain make up the majority of flood disaster victims. During rainy seasons, extreme rainfall from upstream highlands has also harmed large productive businesses and infrastructure (Abdissa & Gudu, 2019).

2.4 Flood Vulnerability Mapping

Flood-prone areas are often dynamic in nature. The nature and degree of vulnerability might change as a country's development progresses (Pradhan & Pirasteh, 2010). They went on to say that the increased level of exposure of the elements under threat makes flood vulnerability worse. There are times, for example, when infrastructure or other structures are built in an area that is already prone to flooding, putting them in a vulnerable zone.

There are also cases where assets and infrastructures are deemed to be outside the sensitive region at the time of construction, but as urban growth progresses, novel consequences emerge from shifting land uses (Pradhan & Pirasteh, 2010). These can include increased rates of runoff, lack of drainage system; the overwhelming amount of rainfall leading to an overflow, and the channelization of rivers which may reduce the amount of discharge they can accommodate (Kumar & Sonam, 2020). All of these factors can increase the number of elements at danger of flooding in a given area, making it critical to keep vulnerability maps updated and monitored in order to properly manage flood vulnerability. Decision-makers need up-to-date information to allocate resources appropriately. According to Singh (2021), flood vulnerability mapping comprises the integration of spatial data to delineate the flood-prone area. Nowadays, different hydrological and geospatial technologies are under use for flood vulnerability mapping. The advanced technology of remote sensing and GIS is serving a vital role in flood hazard mapping (Singh et al., 2021).

2.5 Multi-Criteria Evaluation (MCE)

MCE (multi-criteria evaluation) is a method used by decision support systems to analyze potential courses of action based on numerous parameters and select the best-performing solution (Bulti et al., 2017). Multi-Criteria Evaluation is the process of applying a decision rule to a set of alternatives in decision theory. A decision rule is a method for combining criteria to arrive at a specific evaluation, as well as comparing and acting on those evaluations.

A criterion is a basis for making a choice. There are two sorts of criteria: factors and constraints. Factors are usually continuous (such as slope gradient or road proximity factors) and show the relative suitability of different sites (Bulti et al., 2017). MCE is most commonly achieved by one of the two procedures. Different levels of controls over the tradeoff between factors ad the level of th risk assumed in the combination procedure distinguish each method (Dereje, 2017). The first involves Boolean overlay, the simplest form of aggregation, in which all criteria are reduced to logical statements of suitability and then combined using one or more logical operators like intersection (AND) and union (OR). The second is known as a weighted linear combination(WLC) wherein continuos criteria (factors) are standardized to a common numeric range, and then combined using a weighted average.

The result is a continuous mapping of suitability that can be masked by one or more Boolean constraints to accommodate qualitative criteria and then threshold to produce a final decision (Dereje, 2017).

Each standardized factor map (i.e., each raster cell within each map) is multiplied by its factor weight in the weighted linear combination aggregation method, which then sums the results (Ogato et al., 2020). The resulting suitability map will have the same range of values as the standardized factor maps that were used because the set of factor weights for an evaluation must sum to one. This result is then multiplied by each of the constraints, in turn, to "mask out" unsuitable areas. All of these steps could be completed with the Image Calculator or a combination of SCALAR and OVERLAY. In contrast to the Boolean overlay, the weighted linear combination was used in this study, which gives the continuous level of hazard and risk maps.

De Brito (2018) researched reviewing the application of the MCE method for flood hazard and risk assessment. They have systematically analyzed a total of 128 peer-reviewed papers published from 1995 to June 2015. Results showed that the number of floods MCDM publications has exponentially grown during this period, with over 82 % of all papers published since 2009. They have identified a wide range of applications, with most papers focusing on ranking alternatives for flood mitigation, followed by risk, hazard, and vulnerability assessment and they found that MCE is the most widely used approach for flood hazard and flood risk mapping. After 2016, many researchers have also used MCE for flood hazard mapping and risk assessment, (Bulti et al., 2017; Gebeyehu et al., 2018; Hoque et al., 2019; Lingadevaru et al., 2019; Moazzam et al., 2018; Nigusse & Adhanom, 2019; Ogato et al., 2020; Shawky et al., 2019; Tegegne et al., 2018). After reviewing the most relevant and related kinds of literature, the MCE method was selected to perform this study.

2.6 AHP (Analytical Hierarchy Process)

The Analytic Hierarchy Process (AHP) is a math and psychology-based system for organizing and analyzing complicated decisions. By quantifying its criteria and alternative options, and relating those elements to the overall goal, AHP provides a rational framework for a needed decision (Singh et al., 2021). Based on mathematics and psychology, the analytic hierarchy process is a structured method for organizing and analyzing complex decisions. It was developed by Thomas L. Saaty in the 1970s.

When allocating weights for factors, AHP has the advantage of allowing a hierarchical structure of the criteria, which allows users to focus more on specific criteria and sub-criteria (Dereje, 2017). This is critical since a different structure could result in a different ultimate ranking. Criteria having a large number of sub-criteria are given greater weight than those with fewer sub-criteria.

The analytic hierarchy process, which is a structured technique for dealing with complex decisions, will be used in structuring the flood causative factors in the application of multi-criteria decision analysis (De Brito et al., 2018). The AHP, rather than prescribing a correct decision, theoretically assists decision-makers in identifying the option that best suits their needs and understanding of the problem. As a result, AHP is a decision-making strategy based on people's genuine ability to make key decisions. It allows decision-makers to actively participate in exploring all possible options in order to fully comprehend the underlying problems before reaching an agreement or making a decision (Bulti et al., 2017). As a result, the goal of AHP is to evaluate the given alternatives for a specific goal by establishing priorities for these alternatives as well as the criteria that have been chosen.

2.7 Principles of Geographic Information System

A geographic information system (GIS) is a computer-based system that captures, stores, manipulates, analyzes, manages, and displays geographical and geographic data. Geographic information science (Geosciences) is an academic discipline that studies geographic information systems and is a large domain within the broader academic discipline of geoinformatics. The acronym GIS is sometimes used to refer to the academic discipline that studies geographic information systems and is a large domain within the broader academic discipline of geoinformatics (Minh, 2013). In general, any information system that combines, saves, edits, analyzes, shares, and displays geographic data is referred to as a geographic information system. GIS applications are software programs that allow users to create interactive queries, analyze spatial data, edit data on a map, and present the results of these operations. (Singh et al., 2021).

2.7.1 *Flood vulnerability mapping using GIS*

GIS is quickly becoming a significant tool for assessing risk and managing natural disasters. (Singh et al., 2021). Natural hazard mapping can now be generated using these techniques to demarcate flood-prone zones on a map. These kinds of maps will assist civil authorities in quickly assessing the possible impact of a natural hazard and initiating suitable mitigation actions. (Singh et al., 2021). Such information will assist planners and decision-makers in taking positive and timely actions during the pre-disaster phase. It will also assist them with post-disaster activities such as assessing damage and losses caused by flooding.

The use of a geographic information system simplifies the handling and integration of various spatial and non-spatial datasets, automates flood model development, and simplifies risk analysis (e.g., identifying communities, roads, and cultivated areas that may be at risk of flooding at various levels), as well as the efficient development of inundation maps and statistics that can be utilized as a foundation in various stages of flood disaster management (e.g., from preparedness to mitigation) (Santillan et al., 2016). They have been successful in visualizing the extent of flooding as well as analyzing flood maps to generate flood damage estimation maps and flood risk maps.

Geographic Information System was extensively used to integrate different types of spatial data. Information from various maps, aerial photographs, satellite images, and digital elevation models (DEM) was compiled using a Geographic Information System. Census data and other relevant statistical abstracts were also used to make the risk map more oriented to the need of the local inhabitants (Ogato et al., 2020). In recent years, remote sensing technology combined with geographic information systems has become the primary tool for flood monitoring. According to Joy (2019), the definition of flood zones and the preparation of flood hazards and risk maps for vulnerable locations are the primary concerns in this discipline. Because of their heavy reliance on agriculture, river flooding is a major problem in Africa's developing countries, but any attempt at flood estimation or hazard mapping in this region is hampered by the lack of high-resolution DEM (Behanzin et al., 2015)

Flood hazard mapping is a critical component of flood-prone area land use planning. It generates charts and maps that are simple to read and access, making it easier for administrators and planners to identify risk areas and prioritize mitigation/response efforts (Danumah et al., 2016).

2.8 Importance of remote sensing in flood hazard mapping

The practice of detecting and monitoring the physical features of a region by measuring the reflected and emitted radiation from a distance is known as remote sensing (typically from satellite or aircraft). The use of satellite imageries for hazard and risk assessment has become increasingly important as imagery resolutions have improved, as has the possibility of stereo capability and digital image processing methods (Singh et al., 2021).

Before floods, during floods, and after floods, reliable and timely information about flooded areas, river behavior, and configuration is required for planning flood control and related works; however, such information is extremely difficult to obtain through traditional ground surveys. The introduction of satellite remote sensing technology has aided in the mapping, monitoring, and management of floodplains and flood-prone areas (Mohamed & El-Raey, 2020).

According to (Lillesand, 2000 and 2004) Satellite images are available from a variety of sources, which can be combined or used separately to reveal information about the atmosphere and surface. The visible and infrared channels are two of these channels that are commonly referred to as visible and infrared images, respectively. One type of radiometer that measures visible light and produces visible images is the visible image radiometer (just like a camera taking black and white photographs). The visible is sunlight that has been reflected from the Earth or clouds. Infrared images effectively measure the temperature of the cloud's top or, if there is no cloud, the Earth's surface. The images are usually prepared in such a way that cold surfaces appear white and warm surfaces as dark. Because of the adiabatic lapse rate, temperatures in the lower part of the atmosphere normally decrease with height so a high cloud appears white with a low cloud or the earth's surface appearing darker (Alkema, 2004). Unlike visible images, infrared images are available even when there is no sunlight. Two major processing steps need to be performed before using remote sensing satellite images. These are Image preprocessing, and post-processing (image classification)

2.8.1 Image preprocessing

Pre-processing, also known as image restoration and rectification, is used to correct for data distortion caused by a sensor and platform-specific radiometric and geometric distortion (Singh et al., 2021). All image preprocessing procedures must be completed before using remote sensing satellite images for analysis and information extraction. A radiometric correction is used to correct for uneven sensor response across the entire image while a geometric correction is used to correct for geometric distortion caused by the earth's rotation and other imaging conditions (such as oblique viewing). The image can also be altered to fit a particular map projection system. Furthermore, ground control points (GCPs) are used to register the image to a precise map if the precise geographic location of an area on the image needs to be known (geo-referencing) (Kumar & Sonam, 2020).

2.8.2 Image classification

The task of extracting information classes from a multiband raster image is known as image classification. Image classification produces a raster that can be used to create thematic maps. There are two types of classification: supervised and unsupervised, based on the interaction between the analyst and the computer during classification. To classify an image, the supervised classification uses the spectral signatures obtained from training samples. Without the intervention of an analyst, unsupervised classification finds spectral classes in multiband images. This study has employed supervised image classification, which allows the user to create signatures for each feature to classify the image (Kumar & Sonam, 2020).

2.8.3 ESA's Sentinel 2 satellite image

One of the drawbacks of freely available satellite images is, the ability to show the earth's features in great detail. Remote sensing satellite images are freely available with a variety of spatial and spectral resolutions. Sentinel-2 is a European Space Agency (ESA) Earth observation mission that acquires optical imagery at high spatial resolution (10m for blue(0.443-0.49), green(0.490-0.560), red(0.560-0.665), and near-infrared(0.783-0.842 micrometer) bands to 60 m for the remaining bands) over land and coastal waters (Rimba et al., 2017)

Agricultural monitoring, emergency management, land cover classification, and water quality are just a few of the services and applications supported by the mission. Sentinel-2 was developed and is operated by the European Space Agency, and the satellites were built by a consortium led by Airbus Defense and Space. The 10m multispectral images of the sentinel satellite give more detailed information about the earth's features allowing a user to use the image for different land use land cover analyses. For this research, the sentinel-2 image was downloaded from the official website of the Copernicus Program and was used to prepare the land use land cover map of the study area (*Sentinel-2 - Missions - Sentinel Online - Sentinel*, n.d.).

2.8.4 ALOS PALSAR Digital elevation model

A digital elevation model (DEM) is a three-dimensional computer graphics representation of elevation data used to represent terrain on a planet (such as Earth), moon, or asteroid (Azizian & Brocca, 2020). DEMs are the most common basis for digitally-produced relief maps and are frequently used in geographic information systems. The use of DEM entails the analysis of grids, to identify flow direction and accumulation areas, which are then easily, processed with GIS hydrology tools.

For accurate modeling studies, precise drainage boundaries are required. DEM is widely used to determine terrain attributes at any point, such as slope, aspect, and elevation values. There are various applications of DEM, such as delineation of watersheds and streams and the generation of isometric projections of terrain profiles (Cochrane & Flanagan, 2005).

DEMs can be created by interpolating points from a ground survey or by obtaining them from remote sensing images. Many satellite-based DEMs with various spatial resolutions are freely available. The United States National Aeronautics and Space Administration's Shuttle Radar Topography Mission (SRTM) and Advanced Spaceborne Thermal Emission and Reflection Radiometer (ASTER GDEM) projections are among the most popular and widely available elevation data sets (NASA) (Zhang et al., 2019).

The ASTER DEM has a global terrain elevation measurement with a 30-meter interval of resolution. Different remote sensing-based datasets, such as Interferometric Synthetic Aperture Radar, can also be used to create DEMs (InSAR) (e.g., Advanced Land Observing Satellite (ALOS) Phased Array Type L-band SAR (PALSAR). Also, there is the Digital Surface Model (DSM derived from optical tri-stereo ALOS Panchromatic Remote Sensing Instrument for Stereo Mapping (PRISM) imagery (Dereje, 2017).

The Advanced Land Observing Satellite (ALOS) is a Japanese Earth-observation satellite that was launched on January 24, 2006, by JAXA (Japan Aerospace Exploration Agency, Tokyo; formerly NASDA) (Azizian & Brocca, 2020). ALOS DEM is another source of high-resolution digital elevation data (12.5m). Many researchers have been used ALOS DEM for flood-related work.

Azizian (2020) Suggested ALOS DEM is better than other DEM's for flood inundation mapping. In their research work, they found that using ALOS-30m for hydraulic simulation approximately leads to similar results as well as ground-based DEM. Shawky (2019) also evaluated satellite-based DEMs, SRTM (Global) GL1 DEM V003 28.5 m, ALOS DSM 28.5 m, and PALSAR DEMs 12.5 m and 28.5 m, and their derived channel networks/orders. ALOS PALSAR DEM 12.5 m ranked first among the other global DEMs with the lowest root mean square error (RMSE) and mean difference (MD) values of 4.57 m and 0.78 m, respectively, when compared to the LiDAR DTM 12.5 m. PALSAR DEM 12.5 m and ALOS DSM 28.5 m-derived channel networks/orders yielded the highest horizontal accuracy when compared to those delineated from LiDAR DTM 12.5 m and LiDAR DSM 28.5 m, respectively.

Zhang (2019) Evaluated the accuracy of different DEMs for mapping coastal flooding at local and global scales. They examine the ASTER, SRTM, ALOS, and TanDEM-X for the island of Hispaniola by comparing them with GPS and LiDAR measurements. ALOS DEM was found the most accurate DEM than ASTER and SRTM DEM. This shows that it is better to use ALOS DEM than the other for better accuracy.

For this study, ALOS DEM (12.5m) was downloaded for free from the official website of the Alaska satellite facility and used to get the elevation, TWI, slope, and drainage density values of the study area to prepare a flood vulnerable map of the areas within the study area.

2.9 Empirical review

Floods occur in a variety of locations and magnitudes, resulting in a wide range of environmental effects. Flood catastrophes in Ethiopia are caused by land flooding from high rainfall, climate change, and obstruction of drainages with garbage, development of buildings across drainages, inadequate drainage networks, and population growth in urban areas. Remote sensing imagery and geographic information systems can be very useful in identifying the spatial component of floods for management. Remote sensing provides a comprehensive picture of the spatial distribution and dynamics of hydrological events like flooding and erosion (Ouma & Tateishi, 2014).

In Ethiopia, the use of remote sensing and geographic information systems or flood management is still underutilized. The response to the recent flood disasters in most states of the country, which claimed many lives and properties, destroyed many agricultural and farmlands, and threatened ecological biodiversity, demonstrates this. Only detailed knowledge of the expected frequency, character, and magnitude of hazardous events in a given area, as well as the vulnerabilities of people, buildings, infrastructure, and economic activities in a potentially dangerous area, can be used to mitigate flood disasters (Njoku et al., 2018). Multi-criteria decision-making (MCDM) technologies can help in flood risk management. A set of approaches for constructing and assessing options based on various criteria and objectives is referred to as MCDM(Voogd, 1982). These approaches are capable of dealing with the inherent complexity and uncertainty of such problems, as well as the knowledge acquired from various actors' engagement, and so deliver targeted judgments (Yan et al., 2011). GIS and RS technologies play a vital role in flood disaster management. Many studies have been conducted worldwide using GIS and RS to assess the damage and risk of a flood.

Bulti (2017) assessed flood risk in Adama city using GIS-based multicriteria evaluation methods. the research assessed all three dimensions of flood risk level in Adama City using a multicriteria approach. The study involved identification and mapping of flood hazard zones, flood risk mapping by superimposing considered hazard zone with existing land use of the City in Geographical Information Systems environment.

Dereje (2017) also used GIS and a multicriteria approach for assessing a flood hazard in Sibu sire woreda. To do this, he has developed causative factors such as rainfall, drainage density, slope, elevation, soil type, geology, in the GIS and land use land cover Remote Sensing environment using ERDAS Imagine software. His study indicated that 7.26% and 2.16 % of the area of the Sibu Sire Woreda was a very high flood hazard and risk zone respectively. Using Arc-GIS after analysis of the flood hazard and risk depending on their causative factors, he has also applied KAP study to evaluate the awareness level of the Woreda society to the flood disaster by descriptive frequency analysis of SPSS technique and concluded as their preparedness to any disaster is low.

Ogato (2020) used (GIS)-Based multicriteria analysis method to analyze flooding hazards and risk in Ambo Town and its watershed. They have used a weighted linear combination method in the process of criteria map aggregation for both flooding hazard and flooding risk.

Nigusse (2019) utilized Geospatial technology and MCDA for Flood Hazard and Flood Risk Vulnerability Mapping around Adigrat, Tigray Region, Northern Ethiopia. Their methodology involved the generation of Baseline maps using Landsat satellite images, DEM, aerial photographs, rainfall data, and census population data

Asefa (2019) Assessed Flood Risk in Kewet District, Amhara Region, Ethiopia by using Geospatial based and multi-criteria approaches. To do this, they developed causative factors in the GIS and Remote Sensing environment. The findings of the study revealed that 37.62% of the district is under high and very high (extreme) flood risk.

Rimba (2017) examined that Okazaki city is at risk of flooding due to the combined effects of localized heavy rainfall and geographical conditions. They stated that Determining areas prone to flood hazard are one element of flood hazard maps related to disaster management for urban development is necessary. Their study involved the integration of Remote sensing and GIS techniques, and the AHP calculation to determine the flood-prone area in Okazaki city.

Ouma (2014) has used Integrated Multi-Parametric AHP and GIS techniques to map flood risk and vulnerability in Eldoret Municipality, Kenya. They have used an integrated AHP and GIS analysis techniques for modeling and predicting the magnitude of flood risk areas. To prepare a flood risk vulnerability mapping, they have used a multi-parametric approach by considering six causative factors such as rainfall distribution, elevation and slope, drainage network and density, land-use/land-cover, and soil type.

Fadhil (2020) also applied the spatial multi-criteria evaluation method for Flood vulnerability mapping in the Minraleng Watershed, Maros Regency, South Sulawesi. They have applied Spatial analysis in the GIS environment to estimate flood-vulnerable zones using six relevant physical factors, such as rainfall intensity slope, elevation, distance from the river, land use land cover, and soil type. They have selected these factors based on a literature review. (Tegegne et al., 2018) observed that adequate geographic information on hazards and areas vulnerable to hazard is required to be able to prepare for disaster management. Their work aimed to analyze the risks and impact of flooding using the GIS-based Multi-Criteria Evaluation Approach in Dembiya Woreda, Amhara Region, Ethiopia.

Gourav (2020) studied the importance of Flood hazard zoning to map the extent of flooding which is helpful in case of planning any activities nearby river banks and valley portions of the river. They have implemented AHP and GIS techniques for the first time in the Bhagirathi River basin using four physical parameters like the land use land cover, elevation, slope, and distance from the river. They observed by the spatial analysis that the risk is very high up to 350 m distance along both sides of the river terraces. The results of their study estimated that 16.7% area (1028.3 km2) of the Bhagirathi River basin is vulnerable to flood hazards, 46323 populations and 9753 households of 96 villages were identified as hotspots for flood hazard. Rincón (2018) concluded that due to the increase in flood events in recent years, accurate flood risk assessment is an important component of flood risk mitigation in urban areas. They have used AHP and GIS techniques for flood risk mapping in Greater Toronto Area. Their research aimed to develop updated and accurate flood risk maps in the Don River Watershed within Greater Toronto Area. They have used GIS-based multicriteria analysis along with the AHP method to define and quantify the optimal selection of weights for the criteria that contribute to flooding. Dano (2019) used an integrated approach that combines GIS ANP and Remote sensing derived variables for flood susceptibility assessment and mapping in a case study of Perlis Malesia. Abdelkarim (2020) Also used multicriteria decision analysis based on geographic information systems to build a flood hazard map of the study area. They were applied AHP to extract the weights of eight criteria that affect the areas which are prone to flooding hazards, including flow accumulation, distance from the wadi network, slope, rainfall density, drainage density, and rainfall speed.

From the above review, it is evident that the GIS-based multicriteria analysis along with the AHP method plays a vital role in flood-prone area delineation and flood risk analysis. Results of the study of De Brito (2018) showed that the number of floods MCDM publications has exponentially grown during this period, with over 82 % of all papers published since 2009. Thus, this study was used GIS and a multi-criteria evaluation method to prepare Flood Hazard and Risk Map of Jimma town by utilizing relatively high-resolution remote sensing images such as ESA’s Sentinel 2 image (10m) and ALOS PALSAR DEM (12.5m) and meteorological, and socio-economic, data. Most of the remote sensing image used by the previous researcher for a flood hazard and vulnerability mapping was of lower resolution (30m for Landsat images and 30m for DEM). But for this study, relatively high-resolution remote sensing images such as ESA’s Sentinel 2 image (12m) and ALOS PALSAR DEM (12.5m) were used to derive the causative factors in Jimma town. The causative factors of a flood for the study area were selected based on a literature review and field survey on the existing condition.

CHAPTER THREE; MATERIALS AND METHODS

In this chapter, all the data types and sources are discussed to address the stated objective. The following are the key steps in this study's methodology: (a) identifying and selecting the factors and constraints that were used for flood hazard and risk mapping, (b) data and data source, (c) data acquisition, and (d) data analysis methods to create thematic maps for the parameters that affect the flood hazard and risk process. The following sections also detail the step-by-step procedure used to solve the current problem.

3.1 Description of the study area

Jimma Town is one of the biggest and dominant political, economic, cultural, and historical towns in the Oromia region and southern part of Ethiopia, which has been, founded in the late 1830s. Jimma town is locally known as the town of Aba Jiffar. It is situated 350kms from Addis Ababa on the highway of Mettu – Gambella at an altitude of 1620m. geographically; the town is located at 7° 40'N latitude and 36°60'E longitude. Jimma town is situated within the Gilgel Gibe River catchment upstream. Jimma town is bisected by two major rivers; the Awitu, which flows through the center of the town, and Kit, which flows southwestern end of the town. Jimma town is located upstream of the Gilgel Gibe 1 hydropower reservoir in the Gilgel Gibe river catchment (Dibaba, 2018). Locally, Jimma town is drained by two perennial rivers, namely Awetu and Kito, which will be combined near Dedo bridge located towards the southwest tip of the city and pass through Boye Swamp before they join the Gilgel Gibe River. The Awitu River flows down from the upper mountainous catchment, bisecting the center of Jimma town, and the Kito River flows along the western end. The city's core is densely populated, with individual housing in the intermediate and periphery areas. A smattering of settlements is interspersed with unofficial green spaces. The northern part of the town is dominated by coffee plantations, while the southern part is dominated by eucalyptus and other types of tree plantations (Dibaba, 2018). Throughout the year, Jimma town receives moderately heavy rainfall, with annual precipitation ranging from 1450 to 1800mm. According to data from meteorological data, relative humidity was 56.8% and the highest average humidity was observed during the main rainy season. Figure 3.1 below show the location of the study area with Elevation distribution and major streamlines.

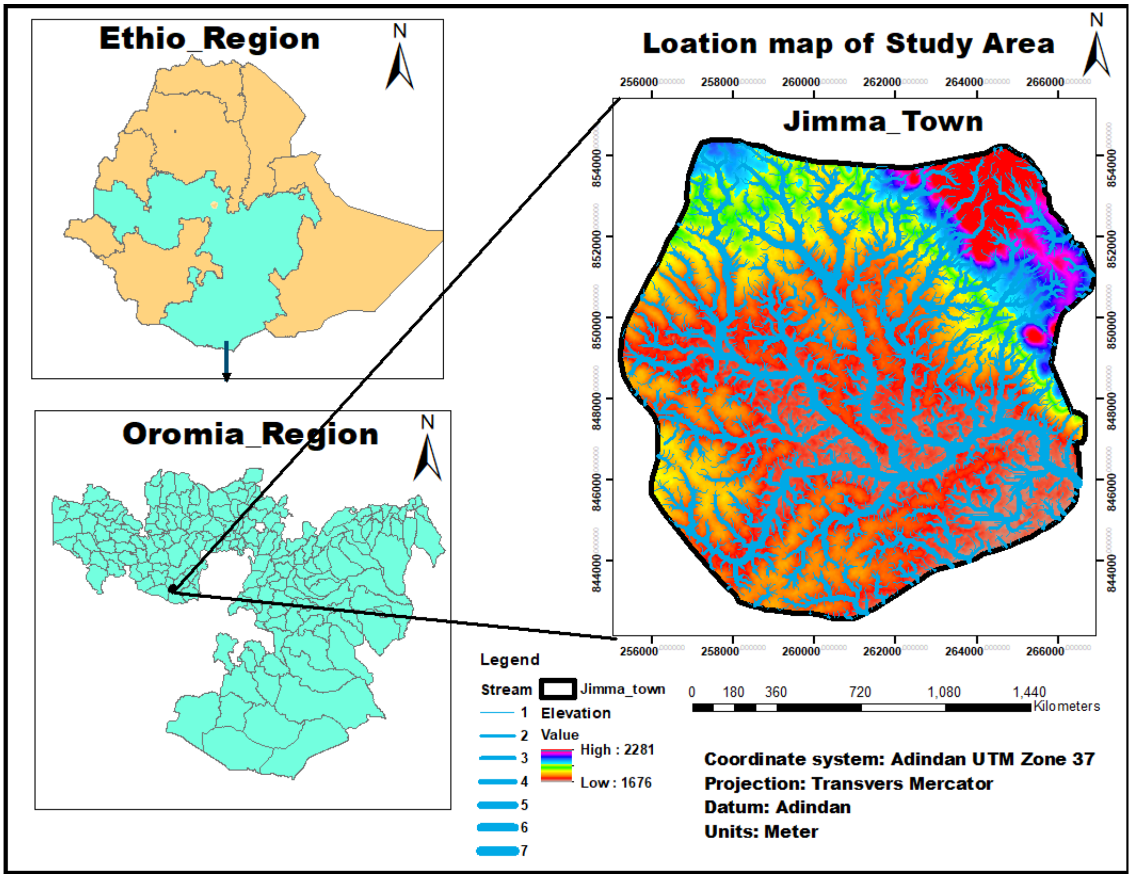

Figure 3.1 Location of the study area

3.1.1 Population

Information on the size of the population of an area has become a very important input. Planning and implementation of any development program require information on the size of the population, the structure of the population distribution of the population density, dependency ratio, and demographic dynamics. To prepare a flood risk map, the population density was used as one important input. Based on the 2007 census conducted by the Central Statistic Agency of Ethiopia, Jimma town has a total population of 120,960. Jimma has a population density of 2,394.30 all are urban inhabitants.

The density of population affects the flood event. The larger the density the more the flood hazard to occur. The gross population density calculation method was used to calculate the number of people per square kilometer. The population shapefile was converted to a raster layer using Conversion Tools/ Feature to Raster. Then further the data layer was reclassified into five classes using a standard classification scheme. In the classification process, an area of high population density is strongly affected by flood and hence ranked to 5, while an area of relatively low population density is the least to be affected by flood and hence ranked to 1.

3.1.2 Precipitation

Jimma city receives moderately heavy rainfall throughout the year, with annual precipitation ranging from 1450 to 1800mm, including more than 100 mm (4 in) per month from April to September (Dibaba, 2018).

Rainfall data from the Seven Metrologic stations, namely Jimma, Chekorsa, Dedo, Jiren Abajifar, Serbo, Somodo, and Yebu have been collected and analyzed. The rainfall pattern is bimodal, with higher rainfall records in the months of March to May and June to September, and lower rainfall records in the months of November to February. Between May and September, the area experiences a long rainy season, during which most of the country's crops are cultivated.

3.1.3 Topography

The terrain in Jimma town is mostly flat and rolling terrain. The city's northern reaches are built on a series of hills or escarpments, with a rolling topography that gradually increases in slope to the north, eventually forming highlands that begin to fall further north in the hinterland areas (Dibaba, 2018). On the other hand, the core areas of the southern part of the city are generally located on a low elevation area of the alluvial plain with a slope further decreasing to the south and southeast.

3.1.4 Soil Condition

Jimma town is mainly covered with black, gray, and red-colored plastic clay soils. Jimma tow soil is formed of residual soils derived from acidic rocks such as Ryholitic rock. Most of the areas surrounding Jimma town are covered by the Rhyolite hills. Most of the depressed areas of Jimma town and its vicinity are formed of firm silty clay material. The soil factor of the study area was derived from the FAO standard classification of Ethiopian soil (Berhanu et al, 2012). There are four types of soils in Jimma town, namely dystric nitisols, Eutric Fluvisols Dystric Vertisols, and Chromic Vertisols. From these four soil types, Eutric Fluvisols cover a larger portion of the study area. To determine their significance in flood generation, their texture was considered.

3.2 Data source and material

This section discusses the data needed for the study as well as the causative factors for flood hazards and risk. It also includes the software necessary for the study such as Arc GIS software, ERDAS IMAGINE- 2015, IDRIS-32, and MS Words. For this research, secondary data sources were used. The secondary data source involves sourcig information from existing records which includes, rainfall data and population data. The lists of materials and software that were used for the accomplishment of the study are tabulated as follows in table 3.2 shown below.

Table 3.1 Data sources

A. Data		**Purpose**	**Sources**
1	ESA's Sentinel image	Land use land cover preparation	(https://scihub.copernicus.eu/dhus/#/home)
2	ALOS PALSAR DEM	To get Elevation, slope values, Topographic wetness index, and drainage lines.	https://search.asf.alaska.edu/#/
3	Population data	To develop a flood risk map	CSA
4	Soil Type	To prepare flood hazard map	Ministry of Agriculture
5	Rainfall data	To prepare flood hazard map	NMA
B. Software used		**Version**	**Purpose**
ArcGIS		10.8	Database creation and preparation of thematic layers, Integration and management of spatial information, weighted overlay analysis.
ERDAS IMAGINE		2015	For image processing for preparation of land use land cover.
IDRISI-32			Eigenvector computation for the selected factor

3.3 Methods

In this study to analyze the risk of flooding in the study area, the general risk equation given by Shook (1997) was used.

Risk= (element at risk) ∗ (hazard ∗ vulnerability) ………………………….……… Equation 3.1

To reach the objectives of the study, the most flood causative factors were identified based on literature review, and a thematic layer for each factor was created in the GIS environment by using the data obtained from different sources. The input datasets were organized in a personal geodatabase and then processed to a suitable format, classified, weighted, and analyzed. The selected factors for the study area include elevation, slope, drainage density, land use land cover, distance from the river, soil type, rainfall, and topographic wetness index. All these thematic layers were weighted and reclassified to a common scale.

ERDAS IMAGINE 2015 was used to perform image processing on satellite images to plan land use/cover forms. The input factors for multi-criteria analysis were preprocessed using the flood hazard analysis criteria that were developed. A pair-wise comparison of each factor was conducted using AHP's nine-point scale comparison techniques. Eigenvector for the selected factor was computed using the Weight module in IDRISI-32 software.

After the causative factors were developed, weighted, ad reclassified, the weight overlay analysis was computed in ArcGIS 10.8 to generate a flood hazard map. From the overlay analysis method, weighted linear combinations were used to produce flood hazards and risk maps for the study area. Then, a flood hazard map that sows flood-prone areas was prepared by overlaying the developed, weighted, and reclassified factors. To prepare a flood risk map, many researchers assumed the vulnerability to be one by considering the degree of loss to be total for the whole study area (Ogato et al., 2020). Similarly, for this research, the vulnerability is assumed to be one. If the vulnerability is assumed to be one, the flood risk equation becomes the multiplication of flood hazard and element at risk. Equal weight has been given for these three factors in weight overlay analysis. Then to generate a flood risk map of the study area, elements at risk layer (land use land cover and population density) and the flood hazard map were overlaid using weighted overlay analysis technique in GIS environments. The activity of data processing and methodological flowchart is summarized as follows in figure 3.2 below

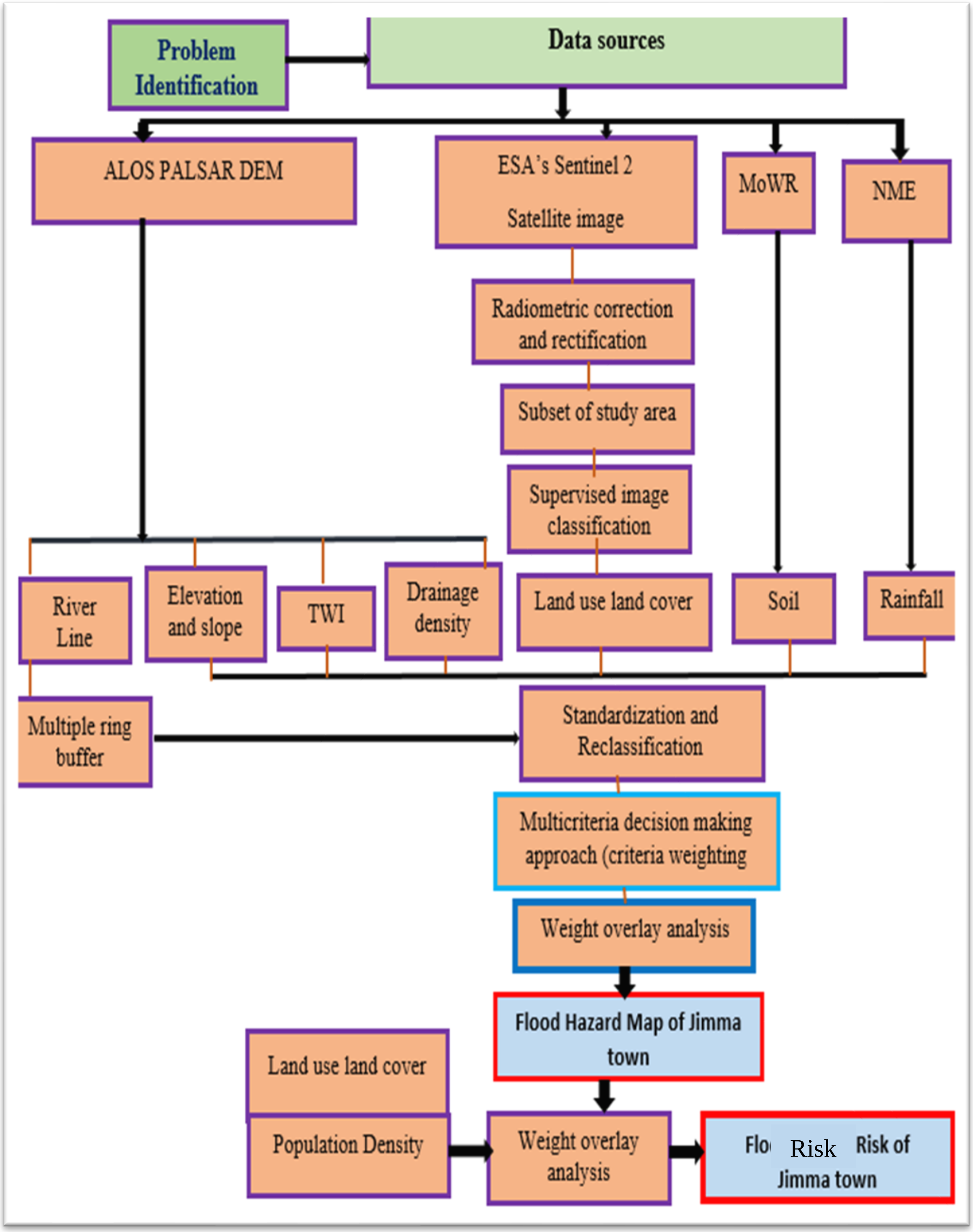

Figure 3.2 Flow chart of the methodology

CHAPTER FOUR; DATA PROCESSING, RESULT, AND DISCUSSIONS

4.1 Introduction

The main objective of this study is to produce a flood hazard and risk map of Jimma town. To prepare this map, eight causative factors were selected for the study area after reviewing different relevant kinds of literature and personal observation and dissection with residents and co-advisor. The selected factors were drainage density, elevation, slope, land use land cover, rainfall, soil type, topographic wetness index, population density, and distance from the river.

All these datasets were organized and standardized in a GIS environment. The vector data layer, soil type was rasterized before being combined to generate identical data layers for GIS analysis. All datasets were stored in a personal geodatabase with a common spatial reference, UTM zone 37.

From these causative factors, drainage density, elevation, slope, land use land cover, rainfall intensity, soil type, topographic wetness index, and distance from the river were used to generate flood hazard map and population density, land use land cover, and the generated flood hazard map were used to prepare flood risk map. To prepare a land use land cover map, a sentinel-2 satellite image was used. The four 10m resolution bands (2, 3, 4, and 8) were layer stacked in ERDAS IMAGINE 2015 software to get the true color composite image. Before image classification, Sentinel-2 satellite image were downsampled to 12.5m spatial resolution to make the spatial dataset cell size equal. The nearest neighborhood resampling method was used in the Arc GIS environment since it is the recommended resampling method for land use land cover mapping

For weighted overlay analysis, weights were allocated for each variable using Satty's Analytic Hierarchy Method, which includes constructing a pair-wise comparison matrix for each map based on a nine-point importance scale(table 4.10). Engine vectors derived from pair-wise comparisons were used to derive weight for each factor. IDRIS selva 32 was used to compute engine vector calculation to derive the weight. The weight of each factor shows how much the factor plays a role in flood hazard occurrence. IDRIS software is a user-friendly software that can perform weight calculations within a second. It also computes a consistency ratio, which indicates if the specified pair-wise weights are acceptable or whether a different arrangement is needed.

4.2 Flood Hazard Causative Factor Development

To generate a flood hazard and risk map for the study area, the selection of the most flood causative factors is important. Although it is difficult to agree on which factors should be used in flood risk assessments, as stated by (Njoku et al., 2018), some important variables play a critical role in flood risk mapping. Authors have used the multicriteria methodology, which combines multiple parameters, over time since it offers a structured approach for evaluating and incorporating the impacts of various variables, involving many levels of dependent, qualitative and quantitative knowledge (Njoku et al., 2018).

The flooding hazard factors for this study were determined by personal observation, and discussion with the co-advisor and chosen primarily based on their theoretical relevance to flood hazards as documented in the literature. The parameters used by Hadipour (2020) were DEM (elevation), flow accumulation, slope chart, population density, land use, ad proximity to the river. Similarly, Kazakis (2015) developed a model that uses seven criteria–parameters to conduct a multi-criteria analysis: flow deposition, rainfall rate, geology, land use, slope, elevation, and distance to the drainage network. Blistanova (2016) took into account rainfall, slope, land use, and soil type. Danumah (2016) looked at a slope, soil. Population density, drainage density, rainfall, and land use. Gashaw (2011) considered slope, elevation, drainage density, soil type, and land use land cover for flood hazard mapping. Bulti (2017) based on the existing condition of their study area, they have selected the five most significant flood causative: land use land cover, drainage density, slope, elevation, and geology. Ogato (2020) was considered land use land cover, elevation, slope, drainage density, soil, and rainfall as important flooding hazard factors in Ambo town’s watershed. Dereje (2017) in his research were used eight interrelated components of the environment as flood causative factors; drainage density, slope, elevation, soil, land use land cover, rainfall, geology, and population density. Abdelkarim (2020) considered six flood causative factors for their study area, such as flow accumulation, distance from the wadi network, slope, rainfall density, drainage density, and rainfall speed.

Furthermore, a comparison of the parameters used by different authors reveals that the geospatial datasets used are similar. Thus, independent variables such as distance from the river, rainfall, elevation, land use/land cover, slope, population density, topographic wetness index, drainage density, and soil type were taken into account for this study.

4.2.1 Drainage Density

Since the density of the water determines the quality of the water, drainage is a critical ecosystem for managing flood hazards. This means that the higher the density, the higher the catchment area is susceptible to flood, resulting in inundation at the lower grounds (Strahler, 1999). Drainage density is one of the main inputs for rainfall runoff, predicting flood levels, and managing water resources. Drainage density is an inverse function of infiltration. Greater drainage density indicates that high runoff for basin areas along with erodible geologic materials (Ouma & Tateishi, 2014). Automation of drainage network extraction from the digital elevation model has received considerable attention. For this study the 12.5m resolution ALOS PALSAR DEM was used to prepare a drainage density map. The first step in the quantitative hazard analysis is a designation of stream order.

To designate stream order, first, the DEM filling was performed in ArcMap spatial analysis tool. Then, flow direction, and flow accumulation processes were performed. Using flow accumulation, stream order was designated. The designated stream orders were converted to line features using the stream to feature tool. The drainage density from the stream order (drainage lines) was then computed using the spatial analyst's line density module. From the polyline features that fall within a radius around each cell, the line density module calculates a magnitude per unit area (Bulti et al., 2017). The density was calculated as a length-to-area ratio. The drainage density of a town is calculated as the length of lines per unit area: D=L/A where D represents the drainage density of the town, L represents the total length of the drainage channels in the town, and A represents the total area of the town.

The Drainage density layer is further reclassified into five subgroups using standard classification schemes namely equal interval (Danumah et al., 2016; Gigović et al., 2017; Mundhe, 2019; Nigusse & Adhanom, 2019). In this classification, the highest drainage density category is ranked to 5 as it has very susceptibility to flooding hazard while the lowest drainage density category is ranked to 1 as it has low susceptibility. Table 4.2 reveals that the drainage density value under 0.822 to 7.935 within the very high level of flood hazard occupies an area of about 137 hectares (1.29 percent). The large portion of the area about 4409 hectares (41.66 percent) occupied between 9.25 and 18.51 of drainage density value. The high flood hazard (11.19 percent) occupies 1183 hectares of the total area.

Table 4.1 Reclassification of Drainage Density of the town

Drainage Density	Ranking	Area in Hectare	% Of Area	Level of Flood Hazard
0.822- 7.93	1	1301	12.19	Very Low
9.25 - 18.51	2	4409	41.66	Low
18.5-27.77	3	3519	33.25	Moderate
27.7-37.03	4	1183	11.19	High
37.3-46.29	5	137	1.29	Very high
Total		**10,583**	**100**	

Likewise, drainage density values ranged from 18.51 to 27.77 covered an area of approximately 3519 hectares (33.25 percent). The area with very high and high drainage density occupies 1320 hectares of the total area (12.48 percent).

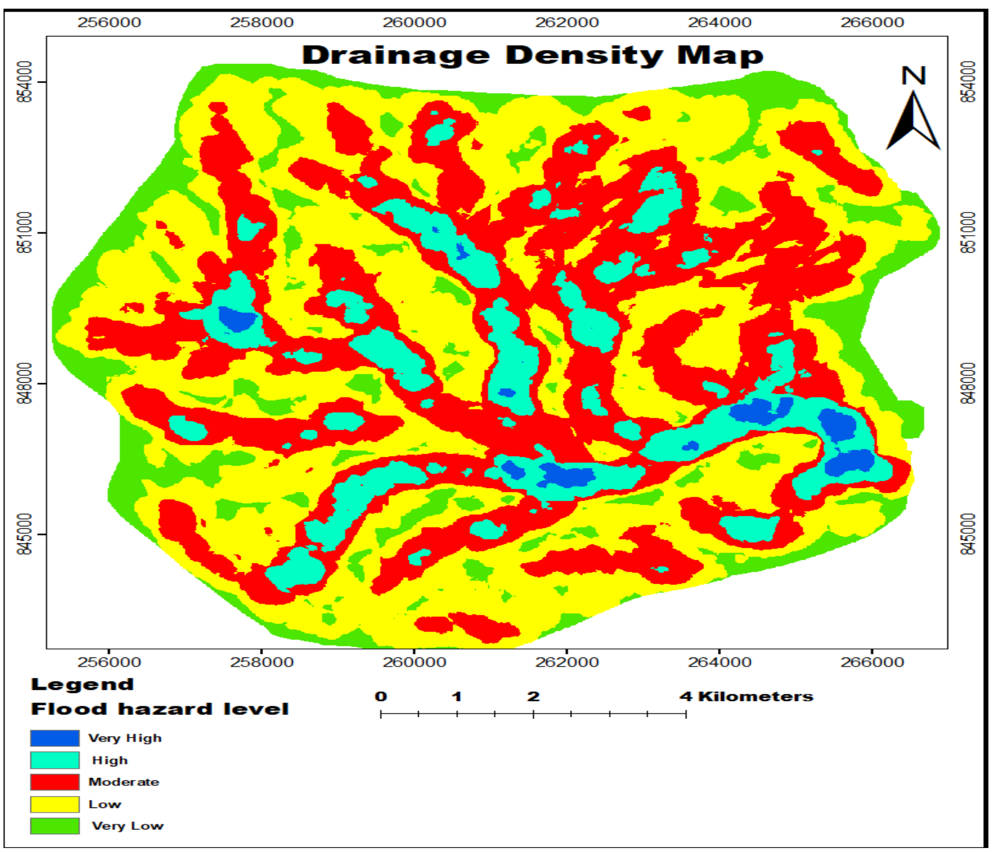

Figure 4.1 Reclassified drainage density map of the town

4.2.2 Rainfall Intensity

Floods are caused by several factors, including heavy rainfall. Flooding is most commonly caused by heavy rainfall that exceeds the capacity of natural watercourses to transport the excess water. Extreme rainfall causes floods, and any water that does not soak into the ground immediately flows downslope as runoff (Njoku et al., 2018). The amount of runoff in a given area is proportional to the amount of rain that falls. The level of water in rivers and lakes rises as a result of heavy rains. When the water level rises above the river bank or dams, the water overflows, causing river flooding. According to Singh (2021), floods or deluges occur when water from rivers, reservoirs, or dams' overflows into areas adjacent to them. The amount of rainfall varies from place to place based on the weather conditions. Thus, the rainfall intensity factor has a significant influence on flooding. To establish continuous raster rainfall data inside and around the town's boundaries, a mean annual rainfall for eleven years (2008–2019) was considered and interpolated using Inverse Distance Weighting (IDW) interpolation method. Rainfall data from the Seven Metrologic stations including Jimma, Chekorsa, Dedo, Jiren Abajifar, Serbo, Somodo, and Yebu have been collected and analyzed. From these rain stations, the station at Jimma town recorded the highest rainfall amount, resulting in a maximum amount of runoff. The resulting raster layer was then reclassified using an equal interval into five classes (Ogato et al., 2020; Ouma & Tateishi, 2014). The reclassified rainfall was assigned a rating ranging from 1 to 5, with 1 being the least rainfall and 5 being the most rainfall.

Table 4.2 Reclassification of Rainfall of Jimma town

Rainfall(mm)	Ranking	Area in hectare	% Of area	Level of flood hazard
1,472.46 - 1,579.71	1	1013.23	9.62	Very Low
1,579.71 - 1,686.22	2	2736.56	25.85	Low
1,686.22 - 1,793.78	3	3111.34	29.39	Moderate
1,793.78 - 1,900.06	4	2132.81	20.14	High
1,900.06 - 2,006.99	5	1569.24	14.82	Very High
Total		**10,583**	**100**	

Table4.2. reviled that the highest rainfall amount with class (1,902.06 - 2,006.99) covers 14.82 percent of the total area. It is evident that 20.14, 29.39, 25.85 percent of the area subjected to high, moderate, and low levels of hazard respectively. From the rainfall map, the central part of Jimma town receives a maximum amount of rain, which indicates it is highly vulnerable to flood hazards. The northern and northeastern parts of the town are under very low and low rainfall amounts. By considering the rainfall amount in northern and northeastern parts, we can say that these areas are less vulnerable to flooding. The results of the raster rainfall layer, IDW interpolated data layer, and reclassified rainfall data are sow in figure 4.2.

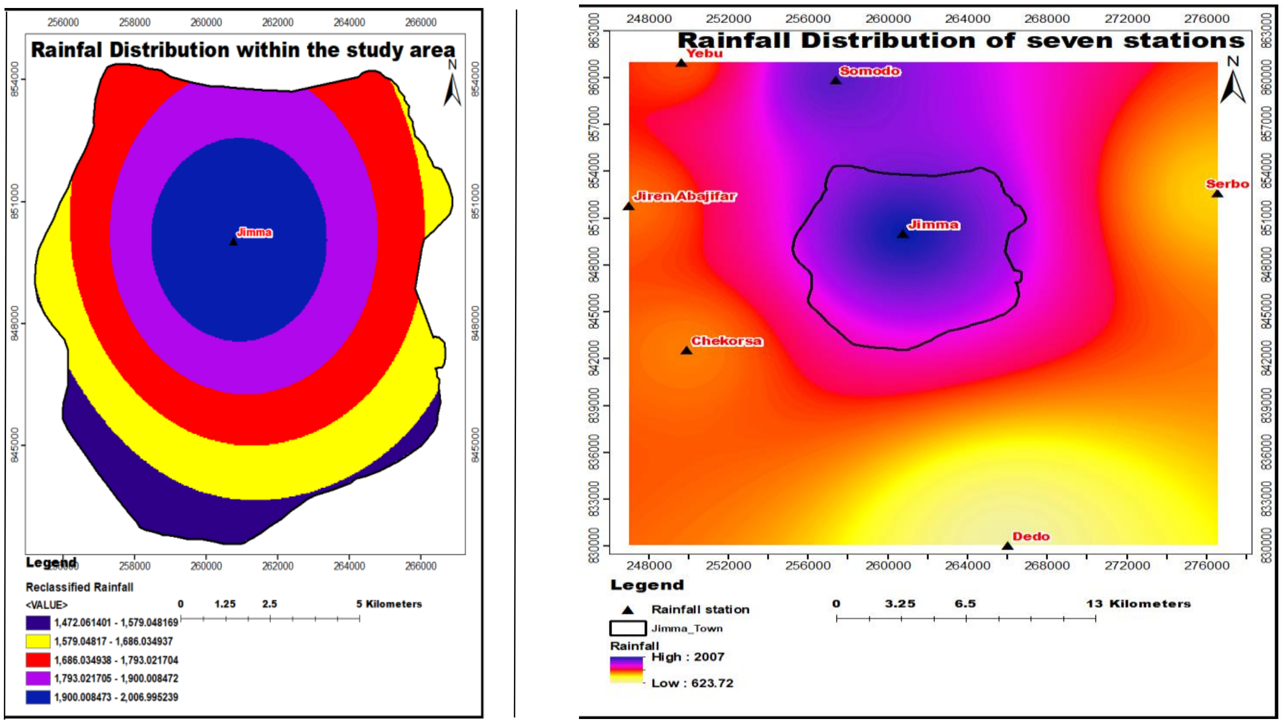

Figure 4.2 Reclassified Rainfall map of Jimma town

4.2.3 Proximity to the River

River overflows are crucial for the initiation of a flood event. Often the inundation emanates from the river and expands into the surrounding areas. Flood vulnerability is highest near river banks and decreases as the distance from the river increases, stressing the significance of distance from the river in assessing flood risk (Kazakis et al., 2015). Locally, Jimma town is drained b two perennial rivers, namely Awitu and Kito. The Awitu River flows down from the upper mountainous catchment, bisecting the center of Jimma town, and the Kito River flows along the western end. The town's main flooding factors were these rivers especially the Awitu river.

According to the previous studies (Fernandez & Lutz 2010), the most affected areas during floods are those areas near the rivers, as the consequence of overflow. Different researchers used different distances from the river to analyze the risk of flooding. Njoku (2018) buffered the river using a 100m buffer interval**.** Muhammad (2019) stated an area up to 600m away from the river is vulnerable to flooding. They used a 600m buffer interval to prepare distance from active river channels. Samanta (2018) also in their research stated that, in March of 2004, on the spate of the Markham River, the riverine zones of Markham were flooded to the brim. To assess the flood risk, they used a 1000m buffer interval. Depending on the capacity of the river channel and the amount of rainfall in the area, the effect of distance from the river will vary. In this study, after reviewing different kinds of literature and considering the previous flood event in the study area, a buffer of 100m interval were prepared to generate distance from the rivers.

Table 4.3 Reclassification of Distance from River of the Jimma town

Distance from River (m)	**Ranking**	**Area in hectare**	**% Of Area**	**Level of Flood Hazard**
0-100	5	935	8.83	Very High
100-200	4	873	8.24	High
200-300	3	813	7.68	Moderate
300-400	2	769	7.26	Low
>400	1	7171	67.75	Very low
Total		**10,583**	**100**	

In this study, after reviewing different relevant literature and considering the previous flood event in the study area, a buffer of 100m interval were prepared to generate distance from the active river. Multiple-ring buffers in GIS ArcMap software were used to prepare the river proximity map. The distance from the river is further reclassified into five classes. The class up to 100meters was assigned the highest Rank as it is more vulnerable to flooding and the class with a distance of more than 400meters was assigned a lower rank. As shown, in table 4.3, the very high and high flood hazard level covers 8.3(935hectare) percent and 8.24 (873hectare) percent of the total area. The reclassified buffered river map is shown in figure 4.3 below.

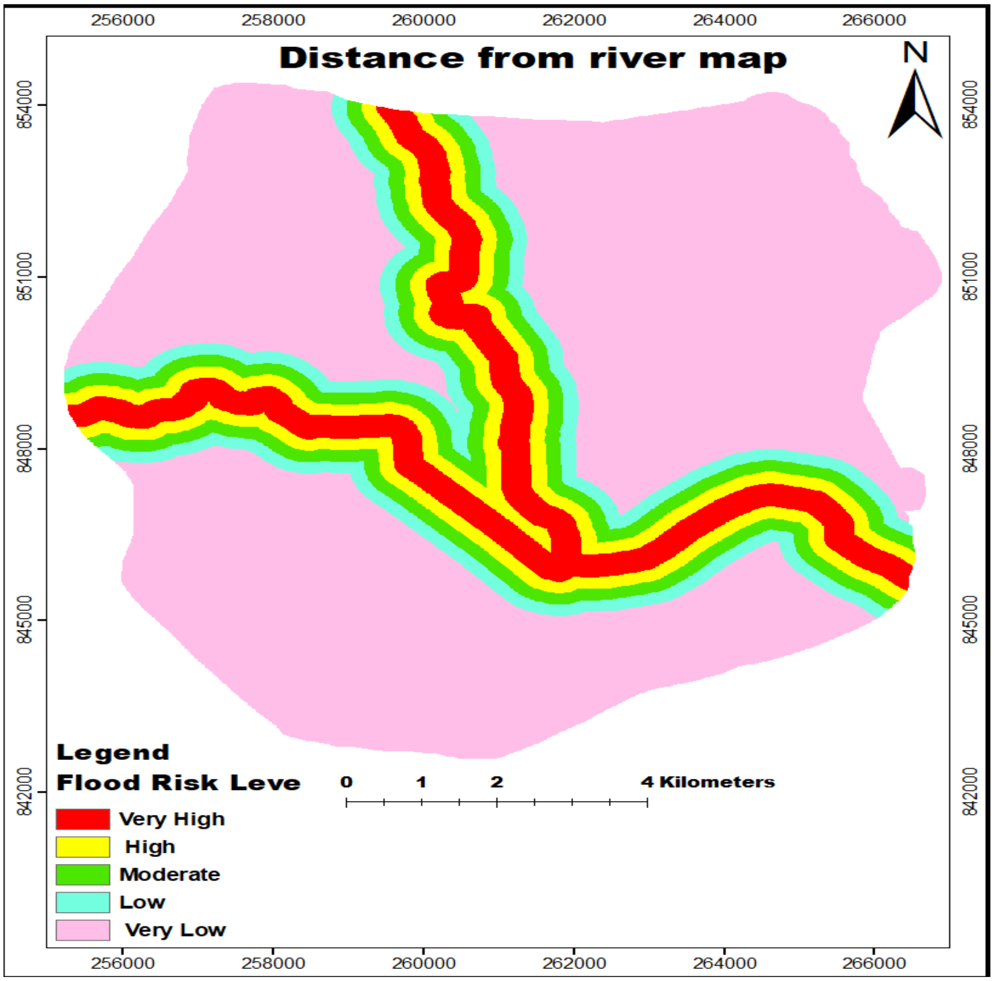

Figure 4.3 Reclassified distance from river map of the Jimma town

4.2.4 Land use Landcover

Land use land cover is also one of the main conditioning factors that strongly contribute to flooding. Water infiltration has a significant influence on the occurrence f floods. Areas covered by vegetation, especially forests have low flood susceptibility because forests have a high infiltration rate (Ouma & Tateishi, 2014). The land use land cover map of the town was reclassified into a common scale in order of sensitivity for the flood risk mapping. Water bodies or wetlands are the most vulnerable areas to flooding since they are covered by water. Science water cannot infiltrate in impervious surfaces, settlements or built-up land uses are also the most flood-prone areas. The passage of water from the sky to the soil is slowed by the thick vegetation cover, which reduces runoff. For this study, a land use land cover map was prepared from a Sentinel-2 satellite image (acquired on 2020-12-27) using ERDAS IMAGINE 2015 software. The four 10m resolution bands (2, 3, 4, and 8) were layer stacked in ERDAS software to get the true color composite image. Before image classification, Sentinel-2 satellite images were downsampled to 12.5m spatial resolution to make the spatial dataset cell size equal. The nearest neighborhood resampling method was used in the Arc GIS environment since it is the recommended resampling method for land use land cover mapping.

A supervised classification method was performed using ERDAS Imagine 15 software and then analyzed using Arc-GIS spatial analyst tool as shown in figure(4.4). The land use land cover map of the town has been classified into five categories, namely vegetation, grassland, farmland, settlements/built-up area, and wetlands. To assess the classification accuracy, a confusion matrix was used by taking 150 points from google earth. The accuracy is essentially a measure of how many ground truth pixels were classified correctly. The overall accuracy of 88.23% was obtained in the accuracy assessment. Land use/land cover types were ranked into different classes based on sensitivity to flooding generation. The higher values were assigned to wetlands (5) and settlements(4) classes and lower values were assigned to dense vegetation areas.

Table 4.4 Reclassification of land use/land cover of Jimma town

Land use/land cover	Ranking	Area in (ha)	% Of Area	Level of flood hazard
Wetlands	5	27	1	Very high
Settlements/Built-up area	4	2899	29	High
Crop Land	3	2566	24	Moderate
Grass Land	2	987	9	Low
Forest/Dense Vegetation	1	4100	37	Very low
	Total	**10,583**	**100**	

From supervised image classification, land use the land cover of the town has five classes, namely wetlands, Settlements/Built-up area, Crop Land, Grass Land, and Forest/Dense

Vegetation having 3, 27, 24, 9, and 39 percent of the total area respectively. From the total area, 1 (27 hectares) and 29 (2899 hectare) percent fall within very high and high flood hazard levels, respectively.

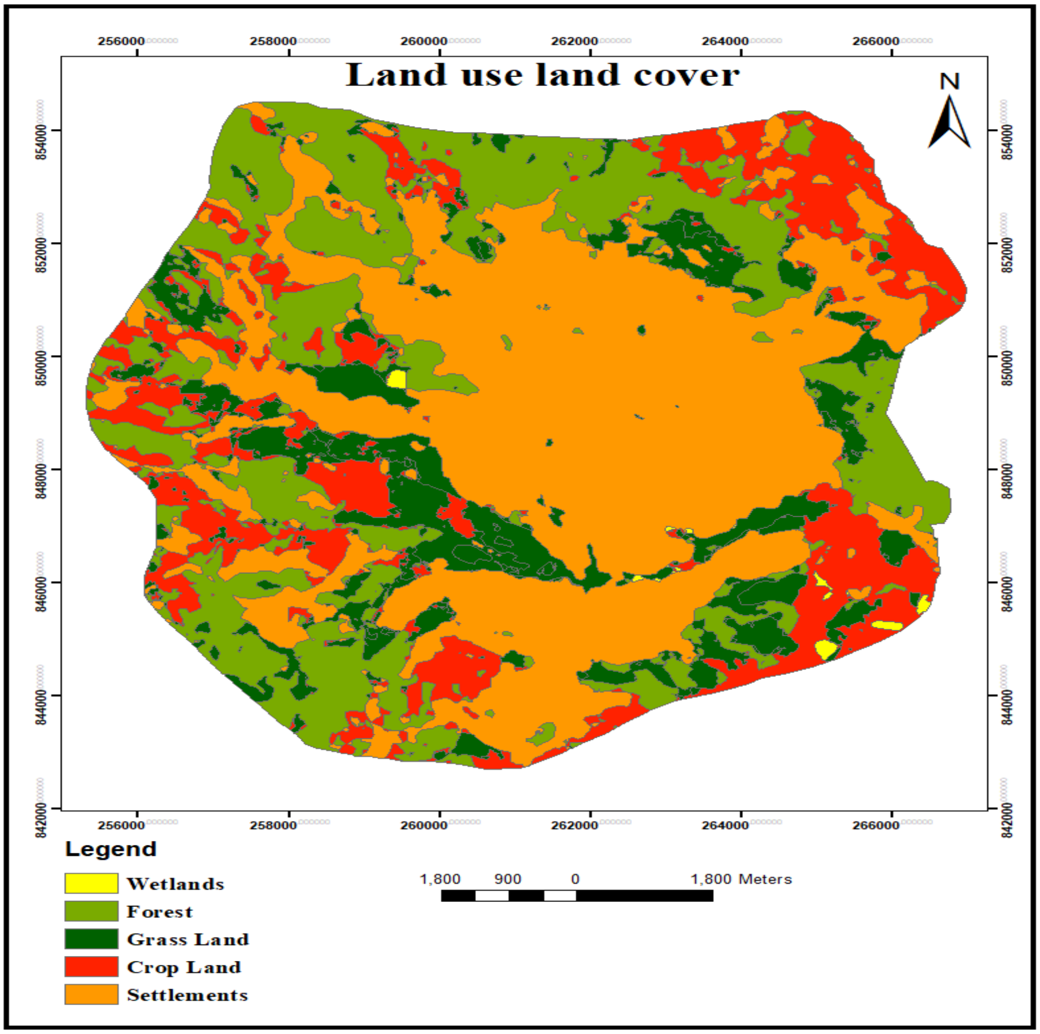

Figure 4.4 Reclassified LULC map of Jimma town

4.2.5 Slope

Areas with less steep slopes may flood more quickly than areas with steeper slopes, which are common in high-elevation areas. The direction and amount of surface runoff or subsurface drainage that reaches a site are influenced by the slope. The contribution of rainfall to streamflow is dominated by the slope (Ouma & Tateishi, 2014). It determines how long overland flow, infiltration, and subsurface flow can last. Slope angles describe the shape of the slope as well as its relationship to lithology, composition, soil type, and drainage. According to

Mohamed (2020), surface runoff is more likely on steeper slopes, while water logging is more likely on flat terrain. Low gradient slopes are extremely vulnerable to flooding when compared to high gradient slopes (Hadipour et al., 2020). Rain or excess river water frequently collects in an area with a poor slope gradient. Flooding occurs when water does not settle in areas with steep slope gradients.

The slope of Jimma town was extracted from 12.5m ALOS PALSAR DEM which was downloaded from the Alaska satellite facility website. The Advanced Land Observing Satellite is a Japanese Earth-observation satellite that was launched on January 24, 2006, by Japan Aerospace Exploration Agency, Tokyo. ALOS DEM is another source of relatively high-resolution digital elevation data (12.5m). Using the Arc-GIS spatial analyst tool, the slope raster layer was further extracted to the town boundary, and the slope was created using the spatial analyst tool raster surface. The slope raster layer was further reclassified into five subgroups using standard classification schemes namely equal interval. This classification scheme divides the range of attributes values into equal-sized subranges, specifying the number of intervals while Arc Map determines where the breaks should be and the new values re-assigned in order of flood hazard rating (Ogato et al., 2020). The classified slope is assigned a value from 1 to 5, with 5 indicating a high influence in the resulting very high flood rate and 1 indicating a very low influence in the resulting very low flood rate (Ogato et al., 2020).

Table 4.5 Slope Range Distributions of Jimma town

Slope (%)	**Ranking**	**Area in hectare**	**% Of Area**	**Level of Flood Hazard**
0 - 9.25	5	7782.2	19.68	Very High
9.25 - 18.51	4	2257.1	20.81	High
18.51 - 27.77	3	361.3	21.67	Moderate
27.77 - 37.03	2	113.4	22.47	Low
>37.03	1	69	15.37	Very low
Total		**10,583**	**100**	

As a result, the slope classes with the highest value were given a lower rank since areas with high slope gradients do not allow water to collect and cause flooding, while the slope classes with the lowest value were given a higher rank due to relatively high run-off. The results of reclassified slope layers are presented in the case study (fig. 4.5)

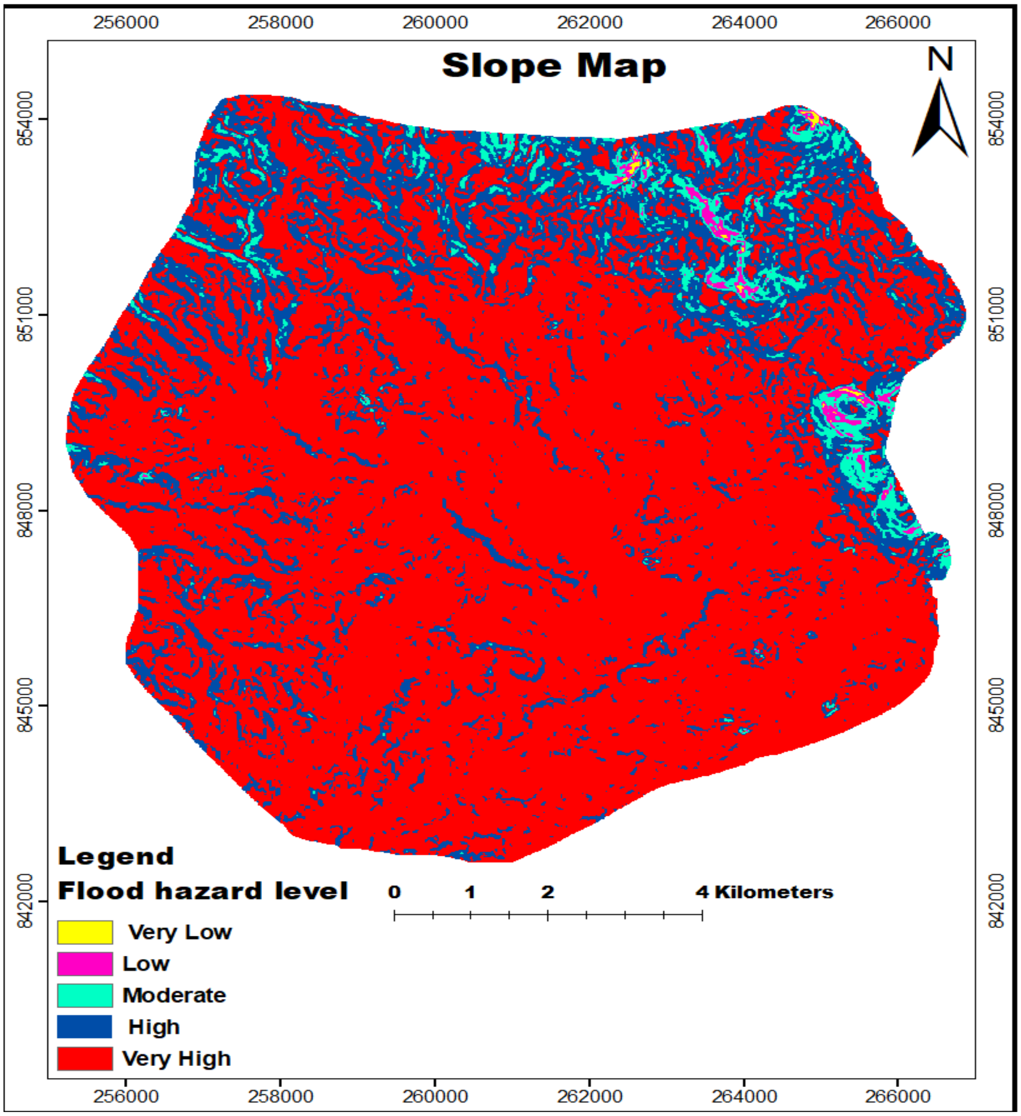

Figure 4.5 Reclassified slope map of the Jimma tow

4.2.6 Soil

Soil water infiltration is used as a flood prediction parameter because it influences the rainfall-runoff process. The most important components and characteristics of soils are soil texture and moisture. Because the sandy soil absorbs water quickly and has few runoffs occurs, soil texture has a significant impact on flooding. On the other hand, the clay soils are less porous and hold water longer than sandy soils, which makes them more vulnerable to flooding(Berhanu et al., 2012). This means that areas with clay soils are more susceptible to flooding. Soil structure and infiltration capacity will have a significant impact on the soil's ability to act as a sponge and absorb water. Soil capacities vary depending on the type of soil (Ouma & Tateishi, 2014). The risk of flooding increases as soil infiltration capacity decreases, resulting in increased surface runoff. When water is delivered at a rate that exceeds the soil's infiltration capacity, it flows down the slope s runoff on sloping land, causing flooding (Ouma & Tateishi, 2014).

The soil factor of the study area was derived from the FAO standard classification of Ethiopian soil (Berhanu et al.,2012). There are four types of soil types are found in Jimma town, namely Dystric Nitisols, Eutric Fluvisols, Dystric Vertisols, and Chromic Vertisols. From these four soil types, Eutric Fluvisols covers a larger portion of the study area. To determine their significance in flood generation, their texture was considered. Chromic Vertisols and Eutric Fluvisols are soil types with clay soil texture, which highly contribute to flooding (Dereje, 2017). Dystric Vertisols and Dystric Nitisols are soil types with a sandy texture, which has relatively less contribution to flooding (Berhanu et al.,2012). The soil group of the study area was converted to a raster format. The soil raster layer was reclassified into four groups, with new values assigned in order of flood hazard rating. Soil type that has a very high capacity to generate a very high flood rate is ranked to highest value and the one with very low capacity in generating flood rate is ranked to lowest value. From the above soil characteristics which are based on water infiltration rate, chromic vertisols are assumed to have a very high flooding capacity and ramked as very high rank (5)

Table 4.6 Reclassification of Soil types of the Jimma town

Soil type	**Ranking**	**Area in hectare**	**% Of area**	**Level of flood hazard**
Dystric Nitisols	1	4537	43	Low
Dystric Fluvisols	2	165	2	Moderate
Eutric Fluvisols	3	5470	51	High
Chromic Vertisols	4	389	4	Very high
Total		**10,583**	**100**	

The soil type of the Jimma town has four categories. They are Dystric Nitisols which covers a large portion 4537 hectare (43 percent) of the total area within Low level of flood hazard, Eutric Fluvisols which about 5470 hectares (51 percent) within a high-level flood hazard, Dystric Fluvisols which covers only 165 hectares (2 percent) of the total area within Moderate level of flood hazard and Chromic Vertisols which covers only 389 hectares (4 percent) of the total area within very high.

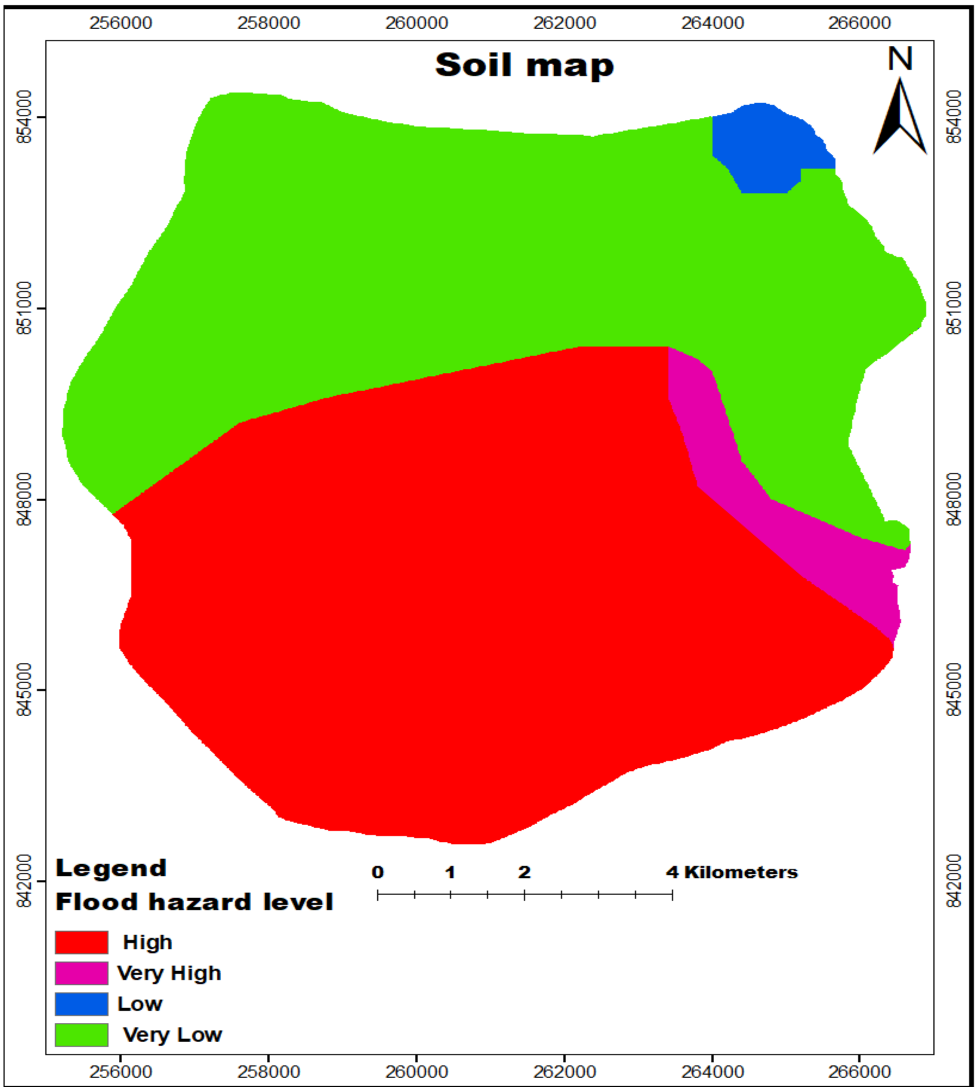

Figure 4.6 Reclassified soil map of the Jimma tow

4.2.7 Elevation

The role of elevation in the spread of flooding is critical. Water flows from higher to lower elevations, and even if other factors that contribute to flooding are in play, the chances of a flood occurring where the elevation is high enough are still slim (Ogato et al., 2020). Low-lying areas are more vulnerable to floods in general. Low gradient slopes and low-lying areas are highly vulnerable to flood occurrences compared to high gradient slopes. Rain or excessive water from the river always gathers in an area where the slope gradient and elevation are usually low. The elevation of the study area was extracted from 12.5meter resolution ALOS PALSAR DEM of the town downloaded from the Alaska Satellite Facility website (https://search.asf.alaska.edu/#/). Elevation of the town was masked by the town boundary in Arc GIS spatial analyst tool.

The slope raster layer was further reclassified into five subgroups using standard classification schemes namely equal interval. This classification scheme divides the range of the values of the attributes into equal-sized subranges, specifying the number of intervals while Arc Map determines where the breaks should be and the new values re-assigned in order of flood hazard rating (Ogato et al., 2020). In this classification process, the lowest elevation category is ranked to the value of 5 as it has a very high susceptibility to flooding hazard while the highest elevation category is ranked to the value of 1 as it has a very low susceptibility to flooding hazard (Fadhil et al., 2020).

Table 4.7 Reclassification of Elevation of Jimma town

Elevation(m)	**Ranking**	**Area in hectare**	**% Of Area**	**Level of flood hazard**
1,676-1,797	5	8085	76.39	Very High
1,797 - 1,918	4	1353	12.78	High
1,918- 2,039	3	758	7.16	Moderate
2,039-2,160	2	302	2.85	Low
2,160-2,281	1	85	0.8	Very low
Total		**10,583**	**100**	

As shown in the above table, Jimma town is categorized into five elevation classes. From the five categories, the very high (8085 hectares) and high (1353 hectare) flood hazard levels cover 88 percent of the total area. It is noted that about 12 percent of the area fall under moderate to very low flood hazard level.

As shown in (Fig.4.7), the elevation of Jimma town ranges from 1676 meters above mean sea level, at some parts of West to central and southern parts of the town, to 2281 meters above mean sea level at the eastern, Northern, and some parts of the north-eastern parts of the town. Generally, all the Western, southern and the central part of the town are having a flat area with little variation in the altitude, whereas some of the Northern and north-eastern areas is a highly rugged area which falls within 2,160-2,281meter elevation. By considering the elevation of the town, we can say that most of south and western parts will be affected by flood hazard since it falls under lower elevation.

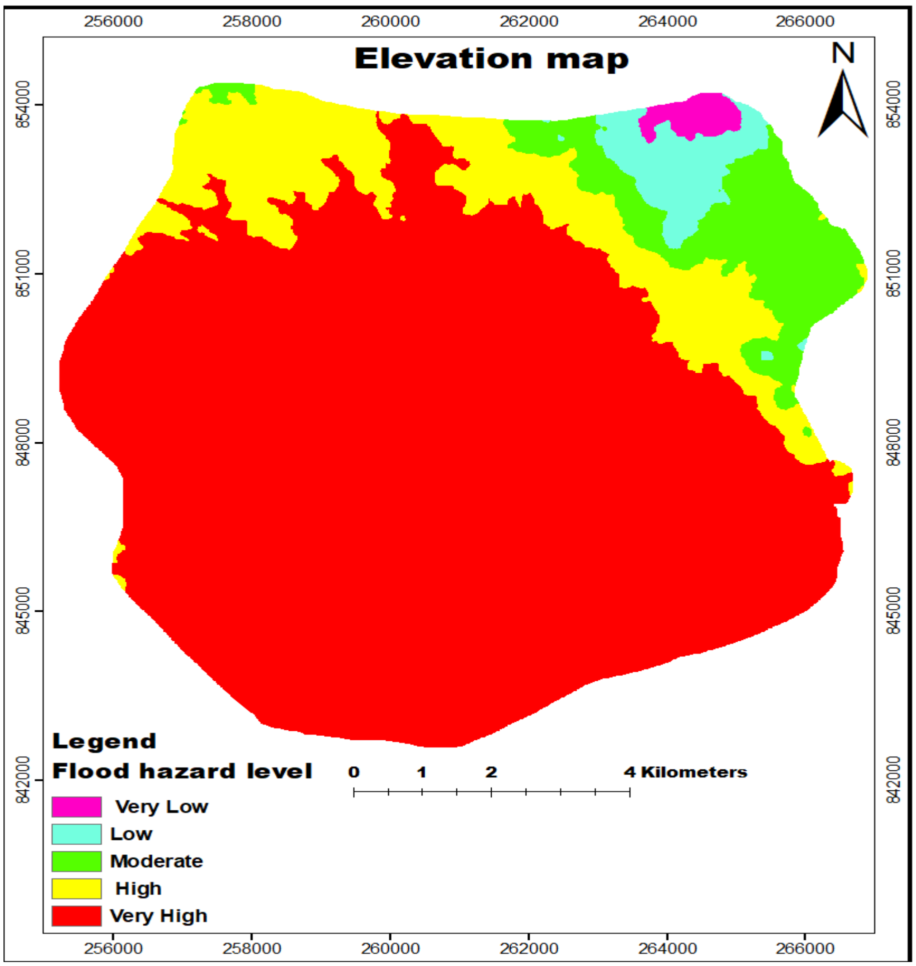

Figure 4.7 Reclassified elevation map of the tow

4.2.8 Topographic wetness index

The topographic wetness index (TWI) controls the overland flow of water by describing the spatial distribution of wetness. TWI has a significant influence on food mapping. (Samanta et al., 2018). The TWI is a physically-based index or indicator of how topography affects runoff, flow direction, and flow accumulation. The index has application in precision agriculture, specialized rainfall-runoff modeling, and simulation of the spatial distribution of soil moisture.

(Qin et al., 2011). A topographic wetness index is based on the idea that a terrain profile controls the distribution of water and areas subject to water accumulation (Samanta et al., 2018). TWI is based on the assumption that the hydraulic slope can be approximated by the topographic slope. There is a strong relationship between TWI and geomorphology as well as the hydrographic position of an area (Counties & Ballerine, 2017; Kumar & Sonam, 2020). This index evaluation is capable of predicting saturated land surfaces that reserves the potential of producing overland flow. For this study, TWI was calculated by evaluating the flow direction, flow accumulation, slope, and various geometric functions derived using GIS software. TWI was calculated based on the formula given by (Beven and Kirkby 1979) and a spatial; distribution map of TWI was prepared using ArcGIS (Fig. 4.8).

$$TWI = Ln\ (a / \tan B),$$

where *a* is the specific catchment area [$a = A/L$, total basin area (A) divided by length of contour (L)], and B is referred to as the slope in degree. The result of the TWI calculation was a GIS data layer that depicts areas with drainage depression where water is likely to accumulate. Smaller values of TWI indicate less potential for the development of ponding; larger values occur where greater upslope areas are drained and the local slope is gentle (Counties & Ballerine, 2017). The TWI layer was reclassified into five classes and the higher value was assigned for the higher TWI and the lower value was assigned for the lower TWI.

Table 4.8 Reclassification of Topographic wetness index of Jimma town

TWI	**Ranking**	**Area in hectare**	**% Of area**	**Level of flood hazard**
2.58 - 6.60	1	6005.78	56.17	Very Low
6.67-10.65	2	3238.60	29.54	Low
10.66-14.66	3	510.362	4.87	Moderate
14.66-18.69	4	374.422	3.7	High
18.69-22.72	5	463.713	4.25	Very high
Total		**10583.21**	**100**	

TWI is useful to demonstrate flood inundated areas due to produced overflow at the time of high precipitation intensity. The higher value of TWI occurs where the higher value of drainage density and lower value of slope exists. Table 4.8. Indicated that 56.17, 29.54, 4.87, 3.7, and

4.25 percent of area respectively subjected to the very low, low, moderate, high, and very high level of flood hazard.

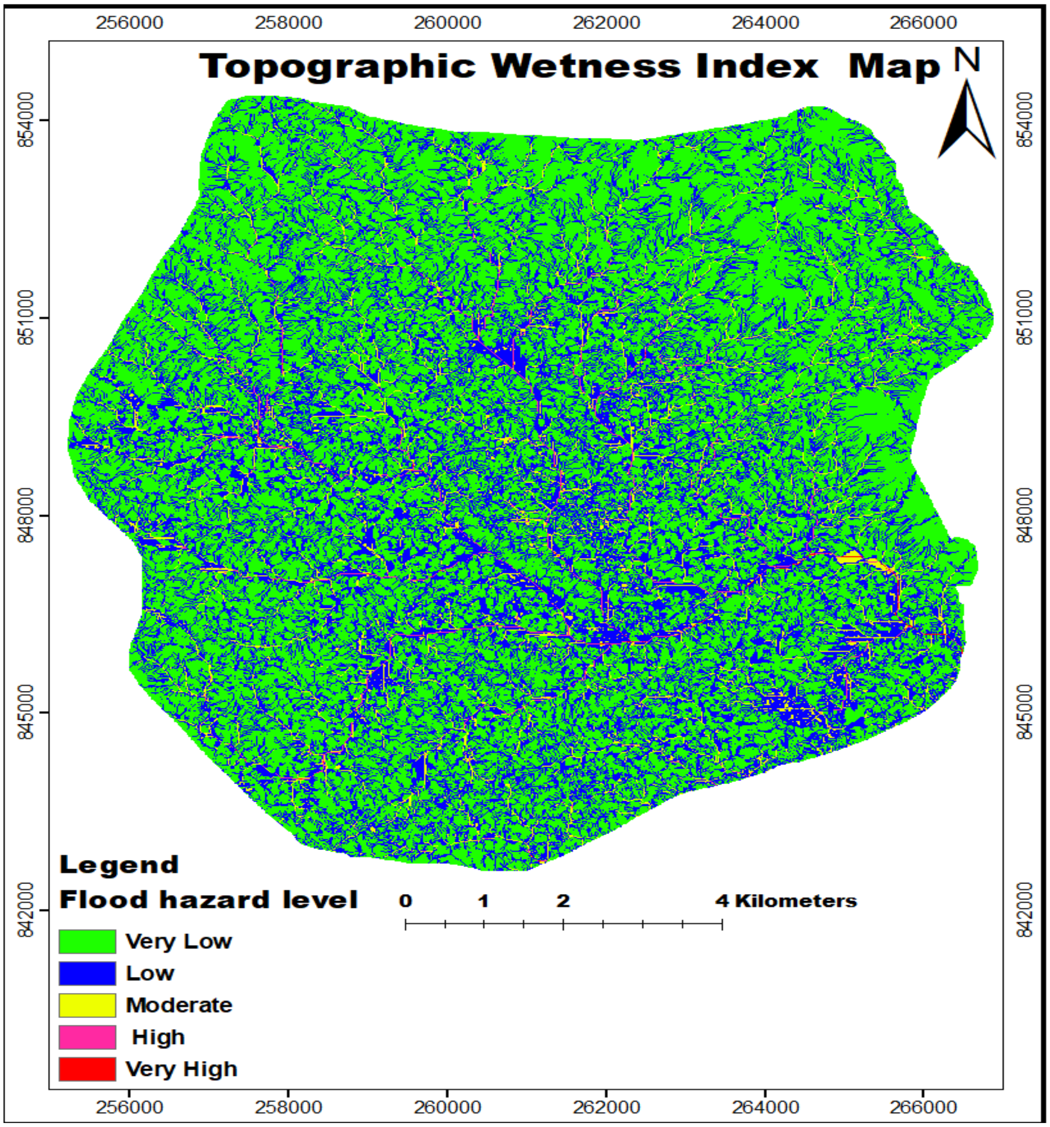

Figure 4.8. Reclassified Topographic wetness index map of Jimma town

4.3 Flood Risk Causative Factor Development

To analyze flooding risk in the study area, the flooding hazard layer and the two elements at risk; population and land use land cover factors were considered as the three important factors. These three factors were overlayed in ArcMap software to determine the degree of flood risk in the study area or to identify the areas within the highest food risk. These three factors were considered to be equally important in the weighted overlay analysis (rating process).

4.3.1 Population density factor

The town's population density was considered one of the flooding risk factors. The impact of the flood is going to harm the population and the man-made infrastructures of the town(Ogato et al., 2020). The population of town data was collected from the census of (CSA2007). The gross population density calculation method was used to calculate the number of people per square kilometer.

The population density layer was further reclassified into five subgroups using standard classification schemes namely equal interval, and new values were assigned in order of increasing flood hazard vulnerability. The population density was reclassified based on the assumption that the denser the population is, the more vulnerable it is to flooding (Ogato et al., 2020). Accordingly, the highest population density category is ranked to the value of 5 as it is very highly susceptible to flooding risk. On the other hand, the lowest population density category was ranked to the value of 1 as it is susceptibility to flooding risk is very low.

Table 4.9 Reclassification of the population density map of Jimma town

Population Density	**Ranking**	**Area in hectare**	**% Of area**	**Level of flood hazard**
0 - 33.4	1	8466.23	80	Very Low
33.40 - 65.8	2	774.91	7.35	Low
65.80 - 98.2	3	465.75	4.59	Moderate
98.20 - 130.6	4	398.32	3.76	High
130.61 – 163	5	450.65	4.25	Very high
Total		**10583.6**	**100**	

From table 4.9, population density value under 0 to 33.4classes within a very low level of flood risk occupies an area of 80 percent. Most of the area falls within a very low flood level. Population density values ranged from 98.20 - 130.6 covered an area of approximately 398.32 hectares (3.76 percent) with a high flood hazard level. The 4.25 percent area recorded a very high population density value between 130.61 – 163 classes within a very high level of flood risk. Figure 4.9 below shows the reclassification of population density based on flood risk zone.

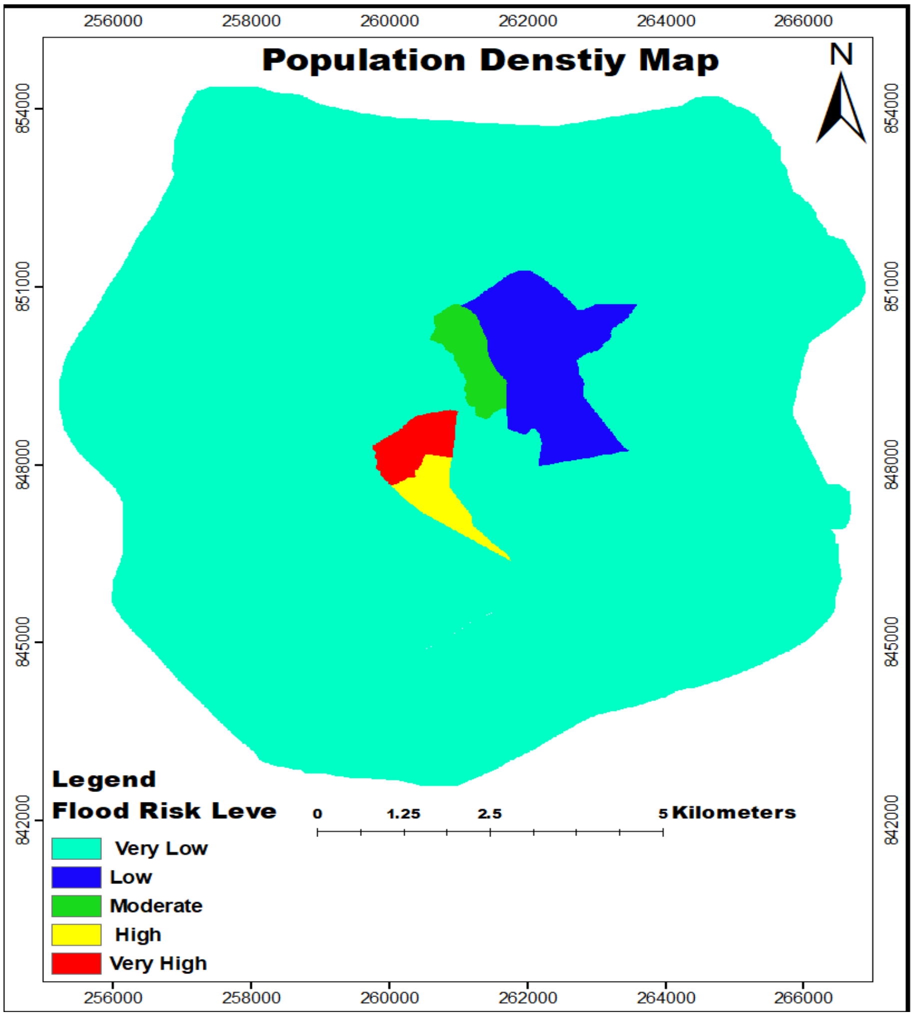

Figure 4.9 Reclassified Population density map of the Jimma town

4.3.2 Land use land cover factor

The cover and use of the land have a different responses to flooding (Ogato et al., 2020). The existing land use classes of the area (water body, built-up, Farmland, grassland, and Dense Forest) of the study area were reclassified into five groups in order of their susceptibility to flooding risk. The land use land cover of the town was reclassified into a common scale in order of sensitivity for flood risk mapping. Water bodies are the most vulnerable areas since they are covered by water. Science water cannot infiltrate in impervious surfaces, settlements or built-up land uses are also the most flood-prone areas. The passage of water from the sky to the soil is slowed by the thick vegetative cover, which reduces runoff. Impermeable surfaces, such as concrete, on the other hand, absorb almost no water. Land use, such as buildings, roads, and slum areas, reduces the soil's penetration capacity and increases water runoff. In other words, land-use types act as water-resistant covers, reducing the time it takes for water to accumulate; and, in most cases, they increase the peak discharge of water, resulting in more severe flooding. This means that land use and land cover are important factors in determining the likelihood of floods (Ouma & Tateishi, 2014).

4.3.3 Flood Hazard Layer

The flooding hazard layer was considered as one of the flooding risk contributing factors in the study area. Very low, low, moderate, high, and very high flooding hazard classes were reclassified based on their susceptibility to flooding risk. A very high flood hazard layer was ranked with a value of 5 as it has the highest susceptibility to flooding risk.. on the other hand, the very low flooding hazard layer was ranked with the value of 1 as it has the lowest susceptibility to flooding risk.

4.4 Data Analysis Techniques

4.4.1 Analytical hierarchy(AHP) weighting process

For this study, the analytical hierarchy process was used for factor weighting by using the Nine points Pairwise comparison scale (Saaty, 1977). AHP has been recognized among researchers, practitioners, and decision-makers for its application in assessing various geo-hazard problems including floods and landslides. Flood risk evaluation is an intrinsically complex multidimensional process including both quantitative and qualitative factors which may be uncertain (Gigović et al., 2017). The main goal of AHP-based multi-criteria decision-making is to rank and prioritize factors. The effectiveness of the available resources, which is, in most cases, the primary judgment of the decision-maker, is directly influenced by the quantity of priority setting. Saaty's analytical hierarchy process is a method for resolving multiple criteria decision problems by prioritizing them. In AHP, a pairwise comparison provides the weight of each causative factor along with a consistency ratio that indicates the level of subjectivity in the factor comparison. AHP was adopted for multicriteria decisions in urban flooding hazard and risk analysis (Bigi et al., 2021; Rimba et al., 2017). In AHP, multiple pairwise comparisons are based on a standardized comparison scale of nine levels (Saaty, 1977). The pairwise judgment is made based on the best information available and the decision-makers knowledge and experience (Gigović et al., 2017; Ouma & Tateishi, 2014). AHP consists of four major steps: problem definition; performing pairwise comparison; calculating the maximum eigenvalues and eigenvectors, calculating the consistency ratio to ensure that the matrix is consistent; and aggregating the relative importance weights for a decision to determine the final weight for decision alternatives (Blistanova et al., 2016; Ogato et al., 2020; Ouma & Tateishi, 2014).

In the multi-criteria evaluation method, the analytical hierarchy process is the most widely used comparison method than the other. All flood causative factors were compared based on their significance to generate more floods. For this study, AHP was used since it offers a flexible, step-by-step, and transparent way of analyzing based on the experts, end-user preferences, knowledge, and judgments.

Table 4.10 Nine-point Pair-wise comparison scale. Source: (Saaty, 1977).

Intensity of Importance	Definition	Explanation
1	Equal importance	Two elements contribute equally to the objective
3	Moderate importance	Experience and judgment slightly favor one parameter over another
5	Strong importance	Experience and judgment strongly favor one parameter over another
7	Very strong importance	One parameter is favored very strongly and is considered superior to another; its dominance is demonstrated in practice
9	Extreme importance	The evidence favoring one parameter as superior to another is of the highest possible order of affirmation
2, 4, 6, 8	Intermediate values between adjacent scale values	
Reciprocals	For inverse comparison	

One of the most significant issues with the AHP method is the requirement to use expert's knowledge in determining weights, which can be considered as a source of bias (Rahmati et al., 2016). The decision of the expert's judgment has a great influence on the final weight of the factors. For this study, However, since all the variables didn't have equal value in determining both flood hazard and risk, determining the variable's weighted influence was done before making modeling. To evaluate the weight of each parameter, a questionnaire on comparisons ratings on a scale of 1-9 (Table 4.10) was prepared and distributed to Tow experts (Geologist, hydrologists) in the area of discipline based on their experience and literature reviews so that variables value impact was easily determined. But, for better criteria weighting, it is highly recommended to increase the number of experts in the area of discipline to participate in the pair-wise comparison. IDRIS 32 software was then used to create a matrix of pairwise comparisons of the criteria for the AHP process based on this 9point scaling method. The pairwise comparisons of all the parameters were used as inputs in the AHP method, and the relative weights of the parameters were used as outputs. The quality of the output of the AHP is claimed to be strictly related to the consistency of the pairwise comparison judgments. The consistency ratio (CR) value was used to assess the pairwise comparison's consistency.

Table 4.11 The pairwise comparison matrix of the factors affecting Flood hazard

	Distance for river	Elevation	Slope	Rainfall	Drainage density	LUL C	Soil	TWI
Distance from river	1							
Elevation	½	1						
Slope	½	½	1					
Rainfall intensity	½	1/3	1/3	1				
Drainage Density	1/3	1/3	1/4	1/5	1			
LULC	1/5	1/4	1	1/3	1/2	1		
Soil type	1/6	1/5	1/5	1/4	1/3	1/2	1	
TWI	1/8	1/6	1/6	1/5	1/5	1/4	1/3	1

From the per-wise comparison, the highest weight was given for proximity to the river (26.11 percent) flowed by elevation (22.09 percent), slope (19.41), Rainfall (13.84 percent). Drainage Density, land use land cover soil, and topographic wetness index obtain 5.27, 3.66, and 2.23 percent of the total weight, respectively. From the derived weight, it is evident that distance from the river factor is the most influential factor in flood generation. This means that the areas near the flood are more vulnerable than the areas far from the river. The eigenvector is used to weight the standardized raster layers to illustrate the importance of each factor in comparison to the other criteria in the resulting flood hazard.

Table 4.12 The Eigenvector of Weights.

The Eigenvector of Weights		**Weight (%)**
Distance from river	0.2611	26.11
Elevation	0.2209	22.09
Slope	0.1941	19.41
Rainfall	0.1384	13.84
Drainage Density	0.0739	7.39
LULC	0.0527	5.27
Soil	0.0366	3.66
TWI	0.0223	2.23
Total:	**1**	**100**
The consistency ratio is 0.06 and consistency is acceptable.		

The consistency ratio (CR) indicates the probability that the matrix rating was randomly generated so that matrices with CR ratings greater than 0.1 should be re-evaluated. In this study, the critical ratio of the calculated Eigenvector is 0.06, which is acceptable. Therefore, each of the parameters can be assigned by these weights.

After the weight for each factor was determined and the consistency ratio is checked, the multicriteria analysis was performed to produce a flooding hazard map by using a GIS environment. In another word, the weighted linear combination method is used in the process of criteria map aggregation. The underpinning reason for imploying WLC is that low scores in one criterion are compensated by high scores in another one in the process of aggregating the criteria flooding hazard map which means the weighted linear combination method multiplies each standardized criteria map with criteria weights, obtaining different variation from the AHP method and then sums the result (Gigović et al., 2017). Accordingly, the flooding hazard map for the town was computed by developing a flood hazard index as shown in Eq.(4.1).

Flooding hazard Index = 0.052*land use/landcover + 0.1941 *slope + 0.15 * soil type +0.1384* rainfall + 0.07 * drainage density +0.22 * elevation + 0.02*TWI + 0.2611 *Distance from river…………………………………………………………. Eq. (4.1)

In weighted overlay analysis, raking, or scaling (from 1 to 5) of each subclass of each factor were performed to determine their significance in flood generation.

Table 4.13 Weighted flooding hazard ranking for Jimma town

Factors	**Weight**	**Classes**	**Rates**	**Level of Hazard**
Distance from river	26.11	0-100	5	Very High
		100-200	4	High
		200-300	3	Moderate
		300-400	2	Low
		>400	1	Very Low
Elevation	22.09	1,676 -1,797	5	Very Low
		1,797 - 1,918	4	Low
		1,918- 2,039	3	Moderate
		2,039 -2,160	2	High
		2,160-2,281	1	Very High
Slope	19.41	0 - 9.25	5	Very High
		9.25 - 18.51	4	High
		18.51 - 27.77	3	Moderate
		27.77 - 37.03	2	Low
		37.03 - 46.29	1	Very Low
Rainfall	13.84	1,511.46 - 1,610.56	1	Very High
		1,610.56 - 1,709.67	2	High
		1,709.67 - 1,808.78	3	Moderate
		1,808.78 - 1,907.89	4	Low
		1,907.89 - 2,006.99	5	Very Low

Drainage Density	7.39	0.822- 7.93 9.25 - 18.51 18.5-27.77 27.7-37.03 37.3-46.29	1 2 3 4 5	Very Low Low Moderate High Very High
LULC	5.27	Water Body Settlements Grass Land Crop Land Dense Forest	5 4 3 2 1	Very High High Moderate Low Very Low
Soil	3.66	Chromic Vertisols Eurtic Fluvisols DystricFluvisols Dystric Nitisols	4 3 2 1	Very High High Moderate Low
TWI	2.23	2.58 - 6.60 6.67-10.65 10.66-14.66 14.66-18.69 18.693-22.722	1 2 3 4 5	Very Low Low Moderate High Very High

Flood risk mapping for the town was done by overlaying the flooding hazard layer, vulnerability, and the two elements at risk; namely population density and land use land cover. Considering the degree of loss to be total for the study area, the vulnerability is assumed to be one. People, economic production, buildings, public infrastructure, cultural assets, ecological species, and landscapes located in a hazardous area or connected to it are all examples of social, economic, and ecological units that are at risk of being affected by various natural hazards in a specific area (Ouma & Tateishi, 2014). The three flood risk factors were considered to be equally important in the weighted linear combination process (Ogato et al., 2020). To prepare the flooding risk map, these three factors were overlaid using the weighted overlay analysis technique in the spatial analyst tool of Arc-GIS 10.8 environment as shown in the methodological flow chart in chapter three figure 3.2. To compute the flooding risk map for the town, a flood risk index was developed and used in a weight linear combination process in the ArcGIS environment as shown in Eq (4.2)

Flooding risk index = 0.3333*Flood hazard + 0.3333*Population Density + 0.3333*Land use/Land cover……………………………………………………………………… Eq. (4.2)

Table 4.14 Weighted flood Risk ranking for Jimma town

Factors	Weight	Classes	Ranking
Flood Hazard of Jimma town	0.3333	Very Low Low Moderate High Very high	1 2 3 4 5
Population Density (Person/Sq.km)	0.3333	0 - 33.4 33.40 - 65.8 65.80 - 98.2 98.20 - 130.6 130.61 – 163	1 2 3 4 5
Land use/Landcover	0.3333	Dense/Sparse vegetation Grass Land Farm Land Settlements Water Bodies	1 2 3 4 5

In this study, for flood risk mapping, only the two elements at risk (population and land use land cover) were considered for weighted overlay analysis. But for a more detailed flood risk assessment, different aspects of vulnerability must be considered (economical, ecological, and social). The vulnerability was assumed to be one, which means an equal degree of loss to flooding risk of element a risk without considering the coping capacity of the persons and structural strength of the buildings. These three factors (land use land cover, population density, and flood hazard map layer) remained to be equally important (33.33 percent for each) in the Weighted Overlay process. The rating of each subclass was done based on their flood generation capacity. A summary of targeted factors, their weights, and ratings are listed in Table 4.14. the information provides in the table was applied to generate the flooding risk map in Jima town. The result from the flooding risk index was the map that shows different levels of flooding risk in the study area, and the map was classified into five risk classes; very low, low, moderate, high, and very high.

4.5 Flood Hazard Mapping and Analysis

Flood disasters are among the most frequent and devastating types of natural hazards in the world. In flood hazard management and mitigation, delineation of the flood-prone areas is the most important task to determine the area's most susceptible to flood hazards. Flooding hazard mapping is a complicated process that integrates different spatial and none-spatial data. For this study, flood hazard mapping was computed by the weighted overlay of all the eight flood causative factors, namely distance from the river, topographic wetness index, slope, elevation, grainage density, rainfall, land use land cover, and soil type. All these factors were developed, reclassified, weighted, and stored in a GIS environment. The weights for each factor were given through discussion with concerned bodies (experts) and based on literature, and eigenvector calculation was performed in IDRIS software. The computed eigenvector was used as a coefficient for the respective factor maps to be combined in weighted overlay analysis in Arc GIS environment for flood hazard and risk mapping.

In this study, the flood hazard maps (Fig 4.10) below show that the detailed results of the flood hazard map of Jimma town were 42.35, 760.96, 6085.54, 2975.19, and 721.60hectare area of Jimma town were subjected to very low, low, moderate, high, and very high flood hazard zone, respectively as shown in (table 4.15).

Table 4.15 Area's coverage of Flood hazard analysis of Jimma town

Rank	Area in hectare	% Of the total area	Level of hazard
1	42.35	0.4	Very low
2	760.96	7.19	Low
3	6085.54	57.49	Moderate
4	2975.19	28.11	High
5	721.60	6.81	Very high
Total	**10,583**	**100**	

Table 4.15. reveals that out of the total 10583 hectare that covers Jimma town, the very high flood hazard zone covers an area of 721.60 hectares while the high flood hazard zone is 2975.19 hectare. The very high flood hazard zone falls around where the maximum amount of rainfall

exists and near the river and within areas with lower elevation. The values for the very high flood hazard zone seem small compared to the total area coverage of the area. However, because floods happened mostly in low lands, and an area with undulating terrain and viable water bodies, people tend to settle at low lands, especially closer to the river. These kinds of human activities are needed to be managed and no developments around the river basin are to be allowed. The flood hazard map of Jimma town also confirmes that, the most flood-vulnerable areas are those areas with low elevation (1,676-1,797m), the area that has a flat slope (0 - 9.25 percent) with clay soil, those areas nearer to the river, and the areas coved by artificial or impervious surface(settlement or built-up areas).

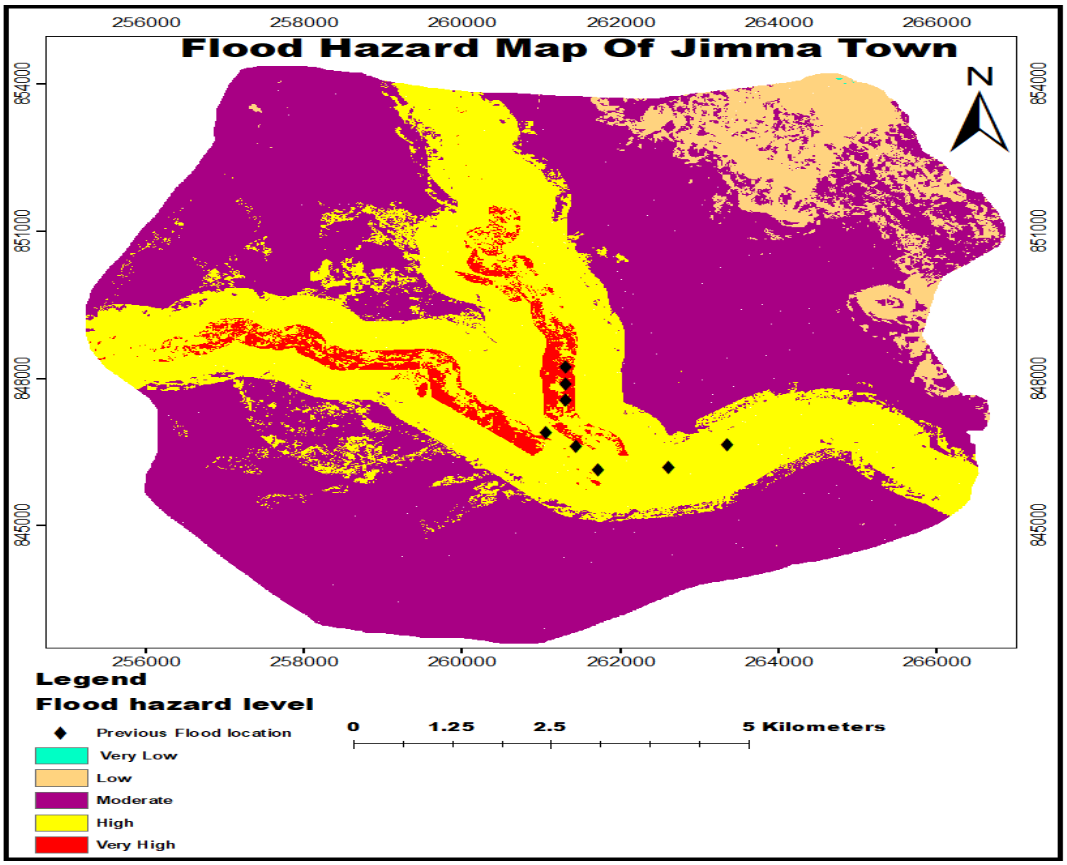

Figure 4.10 Flood hazard map of Jimma town

To get more information to analysis which kebeles of the town is under different level of flood hazard, kebeles were also evaluated in terms of flood hazard level as it is an important domain to administer the population in the Woreda. The detail of the flood hazard level for each kebeles is presented in table 4.16 below.

Table 4.16 Area's coverage(per-kebeles) of Flood hazard analysis of Jimma town.

	Kebele Name	**Flood Hazard**					
		Very low (1)	Low (2)	Moderate (3)	High (4)	Very high (5)	**Total**
		Area in Hectare					
1	BORE	0	0.1562	1186.25	331.7812	0	1,518.18
2	BECHO	0	0	220.4843	293.2812	0	513.76
3	HERMATA MERKATO	0	0	17.8593	280.7031	58.6250	357.18
4	GINJO	0	84.9218	660.9218	2.3437	0	748.18
5	MENDERA KOCHI	0	0	197.0468	44.1406	0	241.18
6	SETO SEMERO	0	251.2343	1114.2343	487.3281	23.4218	1,876.21
7	KOFE	0	0	1354.4531	504.9531	93.0781	1,952.48
8	BOSA KITO	0	0	222.7812	253.8906	37.9843	514.65
9	BOSA	0	0	106.6250	164.1406	26.4843	297.25
10	HERMATA	0	0	0.2031	44.1718	0	44.37
11	GINJO GUDURU	0	0	159.5937	27.546	0	187.14
12	JIREN	421.875	421.6562	397.6875	0	0	1,241.21
13	HERMATA MENTINA	0	0	0	76.5312	8.8437	85.37
14	IFA BULA	0	1.984	843.5000	330.2343	23.859	1,197.59
15	AWEYTU MENDERA	0	0	0	94.5625	11.6406	106.21
16	MENTINA	0	0	0	42.4687	20.2968	62.63
	Total	421.875	759.93	6111.68	2977.95	288.22	**10583.6**

4.6 Flood Risk Mapping

Flood risk mapping was done for Jimma town by taking population density and land use land cover elements that are at risk of flooding combined with the degree of flood hazards of the town. From the flood risk map of the town, it was estimated that 83.49 (0.87 percent), 499.11(4.7 percent), 2762.29 (27.1percent), 3397.60 (32.1percent), and 3839.34 (36.2percent) hectare areas of the town were subjected to very high, high, moderate, low, and very low flood risk levels respectively as shown in (fig.4.11).

The risk elements considered in this study sow different levels of risk. From the existing kebeles in the town, Mentina and Mentina Hirmata kebeles were covered by very high flood risk zone. These two kebeles are located near Awitu river and the area around the place where the previous flood hazard occurred. The Kebeles that are about large hectare their area under high flood risk includes all part Hermata kebele (the central town), almost most of Awetu Mendina kebele, northeastern and south, the southeastern part of Mentina kebele, the southern part of Hermata Merkato kebele, the western part of Baso Kito kebele and northern part of Hermata Mentina kebele as illustrated in figure (4.11). Although, the southern part of Mendera Kochi kebele, the western part of Ginjo Guduru and the eastern part of Kofe kebele were subjected to high flood risk zone.

Table 4.17 Area's coverage of Flood Risk analysis of Jimma town.

Rank	**Area in hectare**	**% Of the total area**	**Level of hazard**
1	3839.34	36.27	Very low
2	3397.60	32.1	Low
3	2762.29	26.1	Moderate
4	499.11	4.71	High
5	83.49	0.78	Very high
Total	**10,583**	**100**	

Table 4.17 reviles that approximately about 0.78 and 4.71 percent of the total area is under very high and high flood risk zone respectively. The moderate flood risk level covers about 26.1 percent (2762.29 hectares) of the total area. The low and very low flood level takes 32.1(3397.6 hectares) and 36.27 percent (3839.34 hectares) of the total area. The flood hazard map of Jimma

town reveals that the central part of the town is under very high and high flood risk. The very high and high flood risk zones are those areas nearer to the river at the center of the town with the highest population density. These areas are, the area around the area near the Awitu river, the area with higher population density, and within the land-use type of settlements/built-up as shown in figure 4.11. The flood risk map of Jimma town also confirmes that, the most flood-affected areas are those areas with low elevation (1,676-1,797m), the area that has a flat slope (0 - 9.25 percent) with clay soil, those areas nearer to the river, an area with higher population density and the areas coved by artificial or impervious surface(settlement or built-up areas).

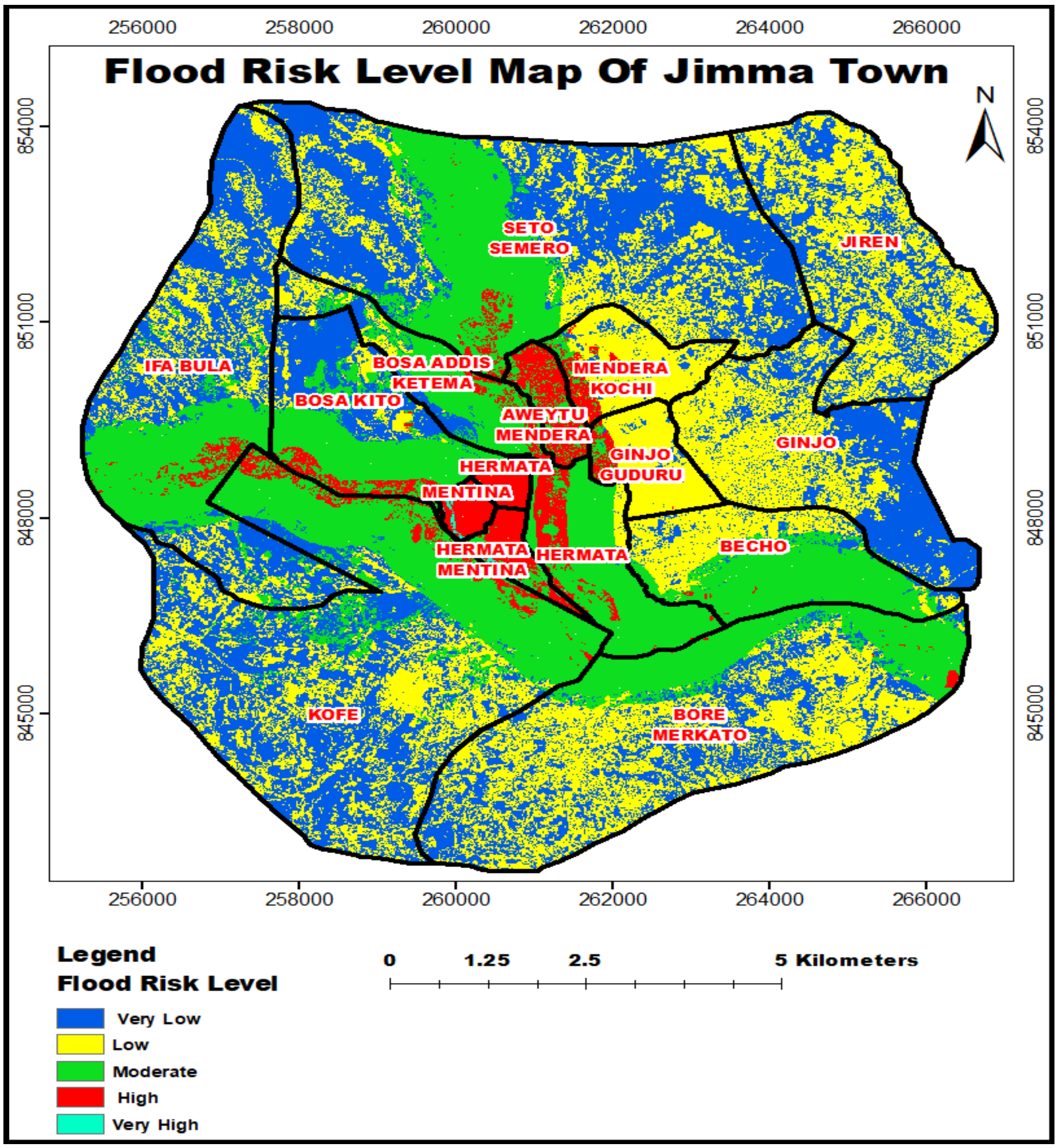

Figure 4.11 Flood risk map of Jimma tow

4.7 Discussions

The flood is one of the most devastating types of natural hazard in the world. The flood hazard can also occur due to how humans are using the existing land. The existence of rivers, inadequate drainage systems, and different activities in the flooded area including deforestation may increase the magnitude of the flood. The spatial variability of flood vulnerability is an important part of flood risk mitigation on the national level, as well as for the application of spatially differentiated approaches to flood defense and mitigation strategy.

This study considered distance from the river, slope, elevation, rainfall, drainage density, land use land cover, soil, and topographic wetness index as important flood causative factors in Jimma town. Flood vulnerability is highest near river banks and decreases as the distance from the river increases, stressing the significance of distance from the river in assessing flood risk (Kazakis et al., 2015). The most affected areas during floods are those areas near rivers,, as a consequence of overflow. Flood mitigation measures need to be taken spacially for the areas adjacent to the river basin. Flooding hazard and risk management experts declared that land use land cover change is one of the major contributors of flooding hazard as urban expansion increases, impervious surface increases, and forest cover decreases in urban areas contributing to an increase in surface runoff (Migosi, 2014). This study also confirms that the most flood-affected areas are the areas that covered by impervious materials or built-up area. Elevation has a key role in controlling the movement of the overflow direction and in the depth of the water level. This study also confirmed the importance of the slope gradient, as it is the major factor in determining the rate and duration of water flow as flatter surface areas are riskier concerning the occurrence of flood concerning the steeper surfaces (Gigović et al., 2017). Soil properties such as soil texture and the degree of moisture in the soil before the rainfall event have a direct impact on the surface runoff process (Ogato et al., 2020). This study also revealed that drainage density plays an important role in flood hazard mapping, as it is an inverse function of infiltration (Ogato et al., 2020). Since the density of the water determines the quality of the water, drainage is a critical ecosystem for managing flood hazards. This means that the higher the density, the higher the catchment area is susceptible to flood, resulting in inundation at the lower grounds (Strahler, 1999).

Urbanization is also asserted to be one of the causative factors for urban flooding risk as the human population in cities and towns in many parts of the world is rapidly growing (Gigović et al., 2017). This study considered the flooding hazard layer, population density, and land use land cover as the three important factors for flooding risk mapping, and these three factors were considered to be equally important in the weighted overlay analysis (Ogato et al., 2020). The result of the research work of (Abdissa & Gudu, 2019) reviled that there is a severe flooding area along the river bank against the return periods. Also, the result of their study indicates that both upstream and downstream right bank of the river is exposed to flooding hence the concerned body should take remedial measures along the river. In this study, the flood hazard map of Jimma town reveals that the central part of the town is under very high and high flood risk. The very high and high flood risk zones are those areas near the Awitu river, the area with higher population density, and within the land-use type of settlements/built-up as shown in figure 5.2. The flood risk map of Jimma town also confirmes that, the most flood-affected areas are those areas with low elevation (1,676-1,797m) (Rahmati et al., 2016), the area that has a flat slope (0 - 9.25 percent)(Kumar & Sonam, 2020) with clay soil, those areas nearer to the river, an area with higher population density and the areas coved by artificial or impervious surface (settlement or built-up areas)(Ogato et al., 2020). The result of this study agrees with the result of the research work of (Abdissa & Gudu, 2019). The developed flood hazard and flood risk maps can help planners and decision-makers to implement adequate strategies to reduce flood impacts. It can also be said that without a detailed flood risk map, it is not easy to delineate the areas at flooding risk, and without a systematic way of making flood risk maps it is not easy to identify the areas at risk.

5 CONCLUSIONS AND RECOMMENDATIONS

5.1 Conclusion

Comprehensive flood vulnerability and risk mapping require detailed information on the field condition, hydrologic statistics, and features of flood defense structures so that probability-based analysis and Comprehensive flood vulnerability and risk Mapping require detailed information on field conditions, hydrologic statistics, and features of flood-defense structures.

In this study, a flood hazard zone map was produced using the analytical hierarchy process-multicriteria evaluation method approach based on the expert's decision and GIS-based analysis for Jimma town. A total of eight flood causative factors were considered in this research based on the local condition and flood vulnerability. Multi-criteria decision-making with the integration of AHP was identified and found very useful for flood hazard and risk analysis offering a flexible, step-by-step, and transparent way of analyzing based on the experts, end-user preferences, knowledge, and judgments. IDRIS selva software was used to compute eigenvector matrix calculation to derive the relative weights for each causative factor. After assigning the derived weights, a flood hazard map of the town was produced using the Flood hazard index in ArcMap 10.8 software. By using the weighted sum method in GIS overlay analysis, the flooding risk map of the town was prepared by overlaying the developed flood hazard map, population density, and land use land cover.

The result of the flooding hazard in Jimma town reveals that 6.81% (721.60hectare), 28.11% (2975.19 hectares), 57.49% (6085.54 hectares), 7.19% (760.96 hectares), and 0.4% (42.35 hectares) of the town is very high, high, moderate, low, and very low flooding hazard zone respectively. The result of the flooding risk in the watershed reveals that 36.27% (3839.34hectare), 32.1% (3397.60 hectares), 26.1% (2762.29 hectares), 4.7% (499.11 hectares), and 0.78% (83.49 hectares) of the town is very low, low, moderate, high and very high, flooding risk zone respectively. Based on the outcome of the study, it could be said that GIS-based Multicriteria analysis offers a simple way to handle complex problems. AHP in combination with the GIS framework can be used as an alternative method while making flood inundation or flood-prone area delineation for flood hazard management.

5.2 Recommendations:

As reported in the records of different kinds of literature, different natural disasters in the past have caused damage to life and property and severely affected the socio-economic status of the region. Sustainable flood risk management in urban areas requires comprehensive flood risk management measures. The following are recommendations:

- Coordination and Implementation Modalities (Federal, Regional, and Wereda Level) must work together. This will aid in the elimination of duplication and the strengthening of mitigation strategies.
- For the areas in lower Elevation, having a positive attitude toward early warning systems is an effective way to reduce flooding risk.
- In flood-prone areas, adequate and sustainable drainage systems should be used because they help to reduce the impact of urban development on flooding and pollution of waterways.
- Flood forecasting and preparedness measures should be implemented as soon as possible to reduce the likely negative effects of flooding on people's lives and livelihoods.
- This research is conducted only to produce a hazard and risk map of Jimma town; Providing information on the major contributing factors, the spatial extent and distribution of flood hazard zones at various levels, and the level of flood risk. Further researches are required to assess the risk of flooding in terms of ecological, social, and economic aspects.
- Additional research is needed to conduct a detailed quantitative analysis at the household level, using a detailed land use function in monetary terms and taking into account additional land-use types and facilities, to get detailed information about flooding risk.
- This study only considered eight flood causative factors to prepare a flood risk map and only three factors to produce a flood risk map. But to prepare a flood hazard map, further studies must be conducted using more flood causative factors (including Geology).
- It is necessary to prepare a Flood Atlas map for all Zones of the country, to use it in flood hazard preparedness. And it is also recommended to assess the flood risk in Jimma town at the watershed level to get more detailed information about the flood hazard in the watershed.

6 REFERENCES

Abdelkarim, A., Al-Alola, S. S., Alogayell, H. M., Mohamed, S. A., Alkadi, I. I., & Ismail, I. Y. (2020). Integration of GIS-based multicriteria decision analysis and analytic hierarchy process to assess flood hazard on the Al-Shamal train Pathway in Al-Qurayyat Region, Kingdom of Saudi Arabia. *Water (Switzerland)*, *12*(6). https://doi.org/10.3390/W12061702

Abdissa, T., & Gudu, F. (2019). *Floodplain Modelling of Awetu River Sub-Basin , Jimma , Oromia , Ethiopia*. *10*(11), 1030–1042.

Akintoye, O. A., Eyong, A. K., Effiong, D. O., Agada, P. O., & Digha, O. N. (2016). Socio-Economic Implications of Recurrent Flooding on Women Development in Southern Ijaw Local Government Area, Bayelsa State, Niger Delta Area of Nigeria. *Journal of Geoscience and Environment Protection*, *04*(08), 33–46. https://doi.org/10.4236/gep.2016.48004

Alkema, D. (2004). Rs and gis applications in flood forecasting. *Management*, 3–4.

Asefa, B., & Mindahun, W. (2019). *Geospatial Based Flood Risk Assessment : The Case of Kewet District , Amhara Region , Ethiopia*. *8*(December 2018), 0–10. https://doi.org/10.5923/j.ajgis.20190801.01

Azizian, A., & Brocca, L. (2020). Determining the best remotely sensed DEM for flood inundation mapping in data sparse regions. *International Journal of Remote Sensing*, *41*(5), 1884–1906. https://doi.org/10.1080/01431161.2019.1677968

Behanzin, D. I., Thiel, M., Szarzynski, J., & Boko, M. (2015). GIS-Based Mapping of Flood Vulnerability and Risk in the Bénin Niger River Valley. *International Journal of Geomatics and Geosciences*, *6*(3), 1653–1669.

Berhanu, B., Melesse, A. M., & Seleshi, Y. (n.d.). *Author ' s personal copy Catena GIS-based hydrological zones and soil geo-database of Ethiopia*.

Bigi, V., Comino, E., Fontana, M., Pezzoli, A., & Rosso, M. (2021). Flood vulnerability analysis in urban context: A socioeconomic sub-indicators overview. *Climate*, *9*(1), 1–18. https://doi.org/10.3390/cli9010012

Blistanova, M., Zeleňáková, M., Blistan, P., & Ferencz, V. (2016). Assessment of flood vulnerability in Bodva river basin, Slovakia. *Acta Montanistica Slovaca*, *21*(1), 19–28. https://doi.org/10.3390/ams21010019

Brunner, M. I., Sikorska, A. E., & Seibert, J. (2018). Bivariate analysis of floods in climate impact assessments. *Science of the Total Environment*, *616–617*, 1392–1403. https://doi.org/10.1016/j.scitotenv.2017.10.176

Bulti, D. T., Mekonnen, B., & Gelaye, M. B. (2017). Assessment of Adama City Flood Risk Using. *Ethiopian Journal of Sciences and Sustainable Development*, *IV*(1), 6–23.

Cochrane, T. A., & Flanagan, D. C. (2005). Effect of DEM resolutions in the runoff and soil loss predictions of the WEPP watershed model. *Transactions of the American Society of Agricultural Engineers*. https://doi.org/10.13031/2013.17953

Counties, D., & Ballerine, C. (2017). *Topographic Wetness Index Urban Flooding Awareness Act Action Support*. *April*.

Dano, U. L., Balogun, A. L., Matori, A. N., Yusouf, K. W., Abubakar, I. R., Mohamed, M. A. S., Aina, Y. A., & Pradhan, B. (2019). Flood susceptibility mapping using GIS-based analytic network process: A case study of Perlis, Malaysia. *Water (Switzerland)*, *11*(3). https://doi.org/10.3390/w11030615

Danumah, J. H., Odai, S. N., Saley, B. M., Szarzynski, J., Thiel, M., Kwaku, A., Kouame, F. K., & Akpa, L. Y. (2016). Flood risk assessment and mapping in Abidjan district using multi-criteria analysis (AHP) model and geoinformation techniques, (cote d'ivoire). *Geoenvironmental Disasters*, *3*(1). https://doi.org/10.1186/s40677-016-0044-y

De Brito, M. M., Evers, M., & Delos Santos Almoradie, A. (2018). Participatory flood vulnerability assessment: A multi-criteria approach. *Hydrology and Earth System Sciences*, *22*(1), 373–390. https://doi.org/10.5194/hess-22-373-2018

Dibaba, W. T. (2018). a Review of Sustainability of Urban Drainage System: Traits and Consequences / Revisão Da Sustentabilidade De Um Sistema De Drenagem Urbana: Características E Conseqüências. *Journal of Sedimentary Environments*, *3*(3), 131–137. https://doi.org/10.12957/jse.2018.37825

Dinh, Q., Balica, S., Popescu, I., & Jonoski, A. (2012). Climate change impact on flood hazard, vulnerability and risk of the Long Xuyen Quadrangle in the Mekong Delta. *International*

Journal of River Basin Management, *10*(1), 103–120. https://doi.org/10.1080/15715124.2012.663383

Ehiorobo, J. O., & Izinyon, O. C. (2011). *Measurements and Documentation for Flood and Erosion Monitoring and Control in the Niger Delta States of Nigeria*. *May 2011*, 14 pp.

Fadhil, M., Ristya, Y., Oktaviani, N., & Kusratmoko, E. (2020). Flood vulnerability mapping using the spatial multi-criteria evaluation (SMCE) method in the Minraleng Watershed, Maros Regency, South Sulawesi. *E3S Web of Conferences*, *153*. https://doi.org/10.1051/e3sconf/202015301004

Fernandez, P., Mourato, S., & Moreira, M. (2016). Social vulnerability assessment of flood risk using GIS-based multicriteria decision analysis. A case study of Vila Nova de Gaia. *Geomatics, Natural Hazards and Risk*, *7*(4), 1367–1389. https://doi.org/10.1080/19475705.2015.1052021

Gashaw, W., & Legesse, D. (2011). Flood Hazard and Risk Assessment Using GIS and Remote Sensing in Fogera Woreda, Northwest Ethiopia. *Nile River Basin*, *6*(9), 179–206. https://doi.org/10.1007/978-94-007-0689-7_9

Gebeyehu, A., Teshome, G., & Birke, H. (2018). *Flood Hazard and Risk Assessment in Robe Watershed Using GIS and Remote Sensing , North Shewa Zone , Amhara Region In Ethiopia*. *23*(8), 34–44. https://doi.org/10.9790/0837-2308033444

Gigović, L., Pamučar, D., Bajić, Z., & Drobnjak, S. (2017). Application of GIS-interval rough AHP methodology for flood hazard mapping in Urban areas. *Water (Switzerland)*, *9*(6). https://doi.org/10.3390/w9060360

Gourav, P., Kumar, R., Gupta, A., & Arif, M. (2020). Flood hazard zonation of bhagirathi river basin using multi-criteria decision-analysis in Uttarakhand, India. *International Journal on Emerging Technologies*, *11*(1), 62–71.

Hadipour, V., Vafaie, F., & Deilami, K. (2020). *Coastal Flooding Risk Assessment Using a GIS-Based Spatial Multi-Criteria Decision Analysis Approach*. *2*(2005).

Hoque, M. A. A., Tasfia, S., Ahmed, N., & Pradhan, B. (2019). Assessing spatial flood vulnerability at kalapara upazila in Bangladesh using an analytic hierarchy process. *Sensors (Switzerland)*, *19*(6), 1–19. https://doi.org/10.3390/s19061302

Jiang, Y., Zevenbergen, C., & Ma, Y. (2018). Urban pluvial fl ooding and stormwater management : A contemporary review of China ' s challenges and " sponge cities " strategy. *Environmental Science and Policy*, *80*(September 2017), 132–143. https://doi.org/10.1016/j.envsci.2017.11.016

Jonkman, S. N., & Dawson, R. J. (2012). Issues and challenges in flood risk management-Editorial for the special issue on flood risk management. *Water (Switzerland)*, *4*(4), 785–792. https://doi.org/10.3390/w4040785

Joy, J., Kanga, S., & Singh, S. K. (2019). Kerala flood 2018: Flood mapping by participatory GIS approach, Meloor Panchayat. *International Journal on Emerging Technologies*, *10*(1), 197–205.

Kazakis, N., Kougias, I., & Patsialis, T. (2015). Assessment of flood hazard areas at a regional scale using an index-based approach and Analytical Hierarchy Process: Application in Rhodope-Evros region, Greece. *The Science of the Total Environment*, *538*, 555—563. https://doi.org/10.1016/j.scitotenv.2015.08.055

Kumar, A., & Sonam, S. (2020). Mapping and assessment of flood risk in Prayagraj district , India : a GIS and remote sensing study. *Nanotechnology for Environmental Engineering*, *1*. https://doi.org/10.1007/s41204-020-00073-1

Lingadevaru, D. C., Jayakumar, P. D., Gs, S., & Vinaya, M. (2019). *Flood Inundation Mappingusing Microwave Remote Sensingand GIS DataIntegration : A Case Study of Tungabhadra and Hagari River Subcatchments in North-East Karnataka , India*. *09*(2), 9–16.

Meyer, V., & Messner, F. (2005). *and Management Methodologies National Flood Damage Evaluation Methods – A Review of Applied Methods in England , the Netherlands , the Czech Republic and Germany*. *November*.

Minh, D. Q. (2013). Application of GIS and Remote Sensing Information for Disaster Risk Management in Viet Nam The Major Natural Disasters in Vietnam. *Regional Workshop on Geo-Referenced Disaster Risk Management System for South-East-East Asia and Pacific, 20-22 February 2013*, *2*, 16.

Moazzam, M. F. U., Vansarochana, A., & Rahman, A. U. (2018). Analysis of flood susceptibility and zonation for risk management using frequency ratio model in District Charsadda, Pakistan. *International Journal of Environment and Geoinformatics*, *5*(2), 140–153. https://doi.org/10.30897/ijegeo.407260

Mohamed, S. A., & El-Raey, M. E. (2020). Vulnerability assessment for flash floods using GIS spatial modeling and remotely sensed data in El-Arish City, North Sinai, Egypt. *Natural Hazards*, *102*(2), 707–728. https://doi.org/10.1007/s11069-019-03571-x

Mundhe, N. (2019). Multi-Criteria Decision Making for Vulnerability Mapping of Flood Hazard: A Case Study of Pune City. *Journal of Geographical Studies*, *2*(1), 41–52. https://doi.org/10.21523/gcj5.18020105

Nigusse, A. G., & Adhanom, O. G. (2019). Flood Hazard and Flood Risk Vulnerability Mapping Using Geo-Spatial and MCDA around Adigrat, Tigray Region, Northern Ethiopia. *Momona Ethiopian Journal of Science*, *11*(1), 90. https://doi.org/10.4314/mejs.v11i1.6

Njoku, C., Efiong, J., Uzoezie, A., Okeniyi, F., & Alagbe, A. (2018). A GIS Multi-Criteria Evaluation for Flood Risk-Vulnerability Mapping of Ikom Local Government Area, Cross River State. *Journal of Geography, Environment and Earth Science International*, *15*(2), 1–17. https://doi.org/10.9734/jgeesi/2018/40527

Ogato, G. S., Bantider, A., Abebe, K., & Geneletti, D. (2020). Geographic information system (GIS)-Based multicriteria analysis of flooding hazard and risk in Ambo Town and its watershed, West shoa zone, oromia regional State, Ethiopia. *Journal of Hydrology: Regional Studies*, *27*(December 2019), 100659. https://doi.org/10.1016/j.ejrh.2019.100659

Ouma, Y. O., & Tateishi, R. (2014). Urban flood vulnerability and risk mapping using integrated multi-parametric AHP and GIS: Methodological overview and case study assessment. *Water (Switzerland)*, *6*(6), 1515–1545. https://doi.org/10.3390/w6061515

Paquette, J., & Lowry, J. (2012). Flood hazard modelling and risk assessment in the Nadi River Basin, Fiji, using GIS and MCDA. *The South Pacific Journal of Natural and Applied Sciences*, *30*(1), 33. https://doi.org/10.1071/sp12003

Pradhan, B., & Pirasteh, S. (2010). *Maximum flood prone area mapping using RADARSAT images and GIS : Kelantan river basin*. *January 2015*.

Process, H. (2019). *Assessing Spatial Flood Vulnerability at Kalapara Hierarchy Process*. 1–

19. https://doi.org/10.3390/s19061302

Qin, C. Z., Zhu, A. X., Pei, T., Li, B. L., Scholten, T., Behrens, T., & Zhou, C. H. (2011). An approach to computing topographic wetness index based on maximum downslope gradient. *Precision Agriculture*, *12*(1), 32–43. https://doi.org/10.1007/s11119-009-9152-y

Rahmati, O., Zeinivand, H., & Besharat, M. (2016). Flood hazard zoning in Yasooj region, Iran, using GIS and multi-criteria decision analysis. *Geomatics, Natural Hazards and Risk*, *7*(3), 1000–1017. https://doi.org/10.1080/19475705.2015.1045043

Rimba, A., Setiawati, M., Sambah, A., & Miura, F. (2017). Physical Flood Vulnerability Mapping Applying Geospatial Techniques in Okazaki City, Aichi Prefecture, Japan. *Urban Science*, *1*(1), 7. https://doi.org/10.3390/urbansci1010007

Rincón, D., Khan, U. T., & Armenakis, C. (2018). Flood risk mapping using GIS and multi-criteria analysis: A greater toronto area case study. *Geosciences (Switzerland)*, *8*(8). https://doi.org/10.3390/geosciences8080275

Samanta, S., Pal, D. K., & Palsamanta, B. (2018). Flood susceptibility analysis through remote sensing, GIS and frequency ratio model. *Applied Water Science*, *8*(2), 1–14. https://doi.org/10.1007/s13201-018-0710-1

Santillan, J. R., Marqueso, J. T., Makinano-Santillan, M., & Serviano, J. L. (2016). Beyond flood hazard maps: Detailed flood characterization with remote sensing, gis and 2D modelling. *International Archives of the Photogrammetry, Remote Sensing and Spatial Information Sciences - ISPRS Archives*. https://doi.org/10.5194/isprs-archives-XLII-4-W1-315-2016

Sanyal, J., & Lu, X. X. (2005). Remote sensing and GIS-based flood vulnerability assessment of human settlements: A case study of Gangetic West Bengal, India. *Hydrological Processes*, *19*(18), 3699–3716. https://doi.org/10.1002/hyp.5852

Sentinel-2 - Missions - Sentinel Online - Sentinel. (n.d.). Retrieved June 16, 2021, from https://sentinel.esa.int/web/sentinel/missions/sentinel-2

Shawky, M., Moussa, A., Hassan, Q. K., & El-Sheimy, N. (2019). Pixel-based geometric assessment of channel networks/orders derived from global spaceborne digital elevation models. *Remote Sensing*, *11*(3). https://doi.org/10.3390/rs11030235

Singh, S., Dhote, P. R., Thakur, P. K., Chouksey, A., & Aggarwal, S. P. (2021). Identification of flash-floods-prone river reaches in Beas river basin using GIS-based multi-criteria technique: validation using field and satellite observations. *Natural Hazards*, *105*(3), 2431–2453. https://doi.org/10.1007/s11069-020-04406-w

Tapia-Silva, F. O., Itzerott, S., Foerster, S., Kuhlmann, B., & Kreibich, H. (2011). Estimation of flood losses to agricultural crops using remote sensing. *Physics and Chemistry of the Earth*, *36*(7–8), 253–265. https://doi.org/10.1016/j.pce.2011.03.005

Tegegne, D., Esa, E., & Nebere, A. (2018). *Flood Hazard Assessment Using Multi-criteria Evaluation Approach in Dembiya Woreda , Amhara Region , Ethiopia*. *5*(December), 18–31.

Voogd, J. H. (1982). Multicriteria evaluation for urban and regional planning. In *Delftsche Uitgevers Maatschappij*.

Yan, H. Bin, Huynh, V. N., & Nakamori, Y. (2011). A probabilistic model for linguistic multi-expert decision making involving semantic overlapping. *Expert Systems with Applications*. https://doi.org/10.1016/j.eswa.2011.01.105

Zhang, K., Gann, D., Ross, M., Robertson, Q., Sarmiento, J., Santana, S., Rhome, J., & Fritz, C. (2019). Accuracy assessment of ASTER, SRTM, ALOS, and TDX DEMs for Hispaniola and implications for mapping vulnerability to coastal flooding. *Remote Sensing of Environment*, *225*(February), 290–306. https://doi.org/10.1016/j.rse.2019.02.028

7 APPENDICES

1. Questionnaire for per-wise comparison
2. The Pair Comparison Matrix of the factors affecting Flood hazard
3. Consistency ratio of the pair-wise comparison
4. Mean Annual Rainfall (mm) of 11Years (Source: NMA, 2020)
5 Total population at kebele level of Sibu Sire Woreda (Source: CSA, 2007).

Adama Science and Technology University

Department of Geomatics Engineering

Appendix 1. Experts based Questionnaire for per-wise comparison

This study entitled **"Flood hazard and risk mapping using multi-criteria evaluation technique and Geospatial technology, a case study Jimma town"** is going to conducted to prepare a flood hazard and risk map of Jimma town using multi-criteria evaluation technique and Geospatial technology by integrating seven flood causative factors namely; **distance from the river, elevation, slope, drainage density, land use land cover, soil and topographic wetness index.** The effect of these independent factors on flooding is different. For weighted overlay analysis, the weight of each factor needs to be determined based on their influence on flood hazards and risk mapping.

The purpose of this questionnaire is to collect survey data for the research study on the "flood Hazard and Risk Mapping using multi-criteria evaluation and geospatial technologies: A case of Jimma town in partial fulfillment of (MSC) degree in Geoinformatics Engineering

This questionnaire is prepared in order to determine the relevance and importance of each factor in flood hazard and risk mapping. **I kindly ask you to compare the flood causative factors based on saaty's 9 points per-wise comparison (table below).**

Thus, I ask you to fill in the information in the table below. The information you provide is used only for the purpose of this study and will be highly confidential.

I would like to thank you in advance for your cooperation!

I. The expert's judgment on flood causative factors (table below)

	Distance from river	Slope	Elevation	Rainfall	Drainage density	Land use land cover	Soil	Topographic wetness index
Distance from river								
Slope								
Elevation								
Rainfall								
Drainage density								
Land use land cover								
Soil								
Topographic wetness index								

II. General Information

Name of the expert: ________________________ **Date** ___________

Profession: _____________________________ **Signature:** ______________

Address: ______________________________

Appendix 2. The Pair Comparison Matrix of the factors affecting Flood hazard

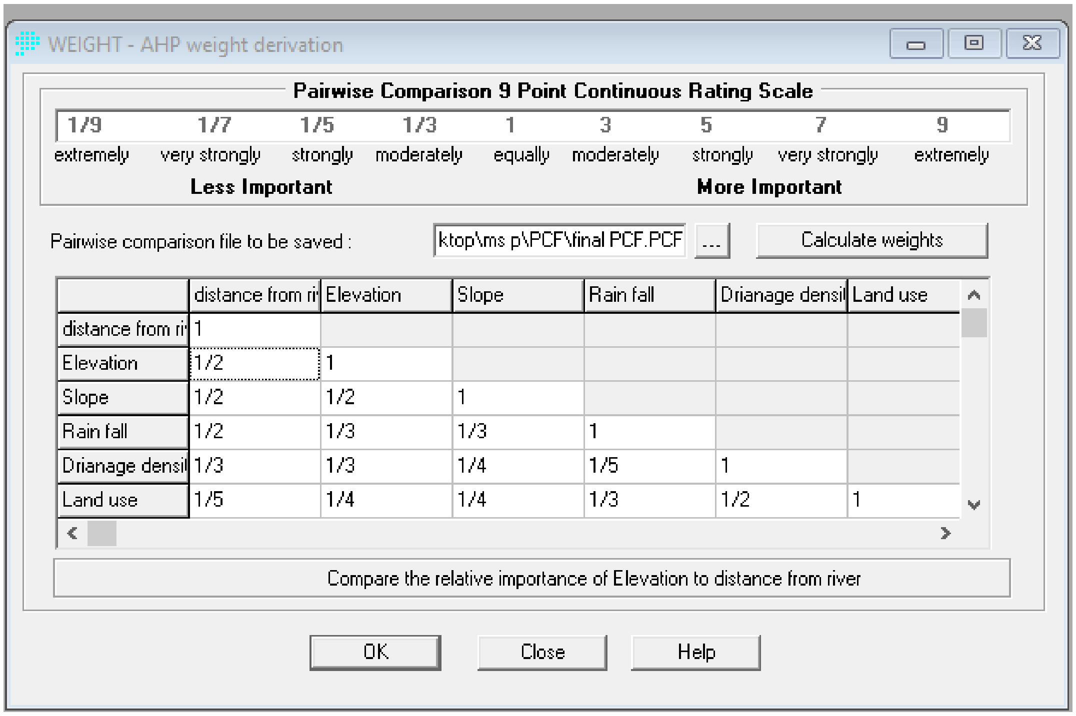

Appendix 3. Consistency ratio of the pair-wise comparison

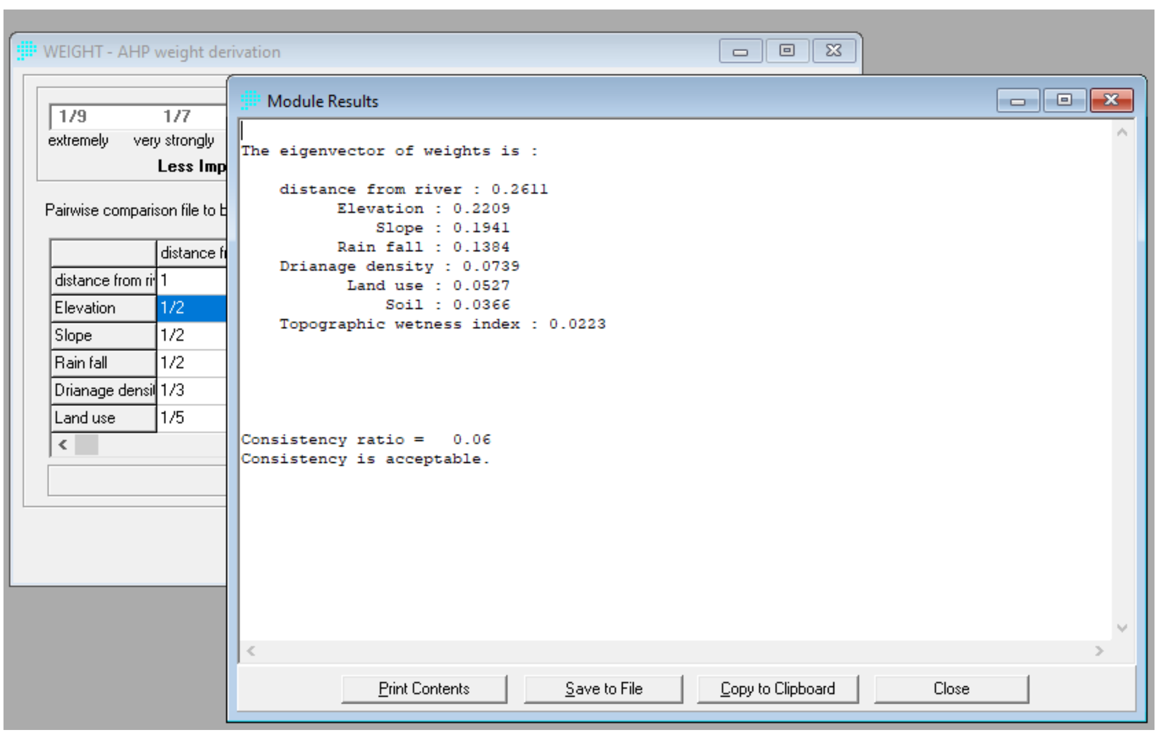

Appendix 4. Population, Households and Housing Units for Urban Kebeles by Sex: CSA (2007)

Geographical Area by name	Total Population			Conventional Households	
	Both Sexes	Male	Female	Households	Housing Units
BOSA ADDIS KETEMA	7,601	3,787	3,814	1,981	1,916
SATO SEMERO	7,444	3,562	3,882	1,774	1,707
MENDERA QOCHI	10,168	5,385	4,783	2,830	2,741
GINJO KETEMA KEBELE	15,940	8,651	7,289	3,954	3,785
JIREN	2,183	1,054	1,129	459	448
BOSO KITO KETEMA	11,000	5,121	5,879	3,143	2,994
MENTINA	7,660	3,629	4,031	2,105	2,026
HERMATA	6,337	3,132	3,205	1,698	1,652
HERMATA MENTINA	9,552	4,773	4,779	2,216	2,069
HERMATA MERKATO	6,160	3,118	3,042	1,522	1,479
AWEYTU MENDERA	9,394	4,446	4,948	2,585	2,505
GINJO GUDURU	8,062	4,164	3,898	2,533	2,280
BECHO BORE	19,459	10,002	9,457	5,391	5,149
KOFE	3856	2223	1633	578	567
IFA BULA	3245	1656	1586	485	472

Appendix 5. Mean annual rainfall (NME)

Station's name	lat	Long	Ele	Mean Annual Rainfall
Jimma	7.67	36.82	1718	2007
Somodo	7.77	36.80	1988	1856.0
Yebu	7.78	36.73	1929	1255.3
JirenAbajifar	7.70	36.70	2008	1208.24
Serbo	7.71	36.97	1802	1045.82
Dedo	7.54	36.88	2281	623.73
chekorsa	7.62	36.73	1770	1179.87